1. Introduction

Ghrelin is an endogenous ligand for the growth hormone secretagogue receptor (GHS-R) [1]. Ghrelin is primarily released from the stomach, but is also secreted from the duodenum and pancreas [1,2]. Peripherally-produced ghrelin influences pituitary hormone secretion, appetite, metabolism, gastrointestinal function, cardiovascular performance, and immune responses. Recently, we characterized ghrelin within the rat hypothalamus [3]; the physiological role(s) of ghrelin secreted from the hypothalamus, however, remains unclear.

Histological analysis indicated that ghrelin receptors localize to a variety of brain regions, including the suprachiasmatic nucleus (SCN) and arcuate nucleus (Arc) within the hypothalamus and the hippocampus [4]. The SCN is important region functioning in the regulation of circadian rhythms, while the Arc plays a primary role in feeding control. The hippocampus has a central role in the regulation of memory. Hypothalamic ghrelin also localizes to the Arc [3]; intracerebroventricular injection of ghrelin induces gene expression of neuropeptide Y and agouti-related peptide and impairs the electrical activity of proopiomelanocortin neurons [5–8]. These results indicate that hypothalamic ghrelin regulates feeding patterns and memory related to feeding.

In this study, we sought to investigate if ghrelin regulates feeding performances by generating ghrelin knockout mice.

2. Materials and methods

2.1. Animal care

All animal protocols were approved by the Ethical Committee for the Research of Life Science of Kurume University. All mice were housed in a 7 a.m. to 7 p.m. light cycle. All experiments were performed with F6 littermate pairs; mice were individually caged during experiments.

2.2. Generation of $ghrl^{-/-}$ mice

These animals will be described in detail in another report. All exons were replaced by a neo cassette. Targeted ES cells and resultant wild-type ($ghrl^{+/+}$), heterozygous ($ghrl^{+/-}$), and homozygous ($ghrl^{-/-}$) pups were genotyped by Southern blot analysis using a 5′-probe, 3′-probe, and exon probe.

2.3. Preparation to tissue and ELISA

To confirm the absence of ghrelin from the stomachs of $ghrl^{-/-}$ mice, tissues were quickly removed after mice were sacrificed. Each sample was diced and boiled for 5 min in a 10-fold volume of water to inactive intrinsic proteases. After cooling, solutions were adjusted to final concentrations of 1 M AcOH and 20 mM HCl. Tissues were homogenized with a Polytron mixer; after centrifugation at 15,000 rpm for 10 min, supernatants were loaded onto Sep-Pak C18 cartridges (Waters, Milford, MA). Cartridges were then washed in 0.9% NaCl and 10% CH_3CN/0.1% TFA before bound peptide was eluted with 60% CH_3CN/0.1% TFA. The eluate was lyophilized and analyzed using an active ghrelin ELISA Kit (Mitsubishi Kagaku Iatron, Inc., Tokyo, Japan).

2.4. Immunohistochemistry

Mice was perfused with 4% PFA solution and embedded in paraffin. Immunohistochemical staining of ghrelin was performed using the avidin–biotinylated-enzyme complex (ABC) method in conjunction with a VECTASTAIN ABC-PO kit (Vector Laboratories Inc., Burlingame, CA). Immunostaining was performed as previously described [3,9]. Briefly, sections were deparaffinized in xylene and a graded series of ethanol. Sections were then pretreated with 3% hydrogen peroxide in methanol for 5 min to endogenous peroxidase activity. After rinsing with PBS, sections were treated for 30 min with 1.5% normal goat serum, then incubated with polyclonal rabbit anti-ghrelin antibody (#6-6; diluted 1:80,000) for 16 h at 4 °C. Sections were rinsed in PBS and incubated with biotinylated anti-rabbit IgG for 40 min. After rinsing in PBS, sections were incubated with avidin–biotinylated regents for 1 h. Sections were visualized with DAB solution (DAKO, Kyoto, Japan).

2.5. The analysis of feeding performance and memory

$Ghrl^{-/-}$ mice were housed in a K2-CABIN apparatus (Phenotype analyzing, Nagasaki, Japan) and given a powder diet (CREA, Tokyo, Japan) to estimate feeding patterns. Animals were given free access to feed and water. Using this system, we recorded the amounts of food and water intake every 15 min for 12 days. To reveal the adaptation capability of mice to a negative energy state, we instituted scheduled feedings. Mice were given feeds for a 4 h period only from 9 a.m. to 1 p.m. We then measured the 4-h food intake at 1 p.m. To investigate memory in $ghrl^{-/-}$ mice, mice were housed in the KUROBOX apparatus (Phenotype analyzing, Nagasaki, Japan) [10].

2.6. Statistical analysis

Results are presented as the means±SD for each group. Comparisons between groups were made using ANOVA with a Williams test. $P<0.05$ was accepted as statistically significant.

3. Results

3.1. Target disruption of the ghrl locus

Loss of the *ghrl* allele was confirmed by southern blot and PCR analysis of DNA isolated from $ghrl^{+/+}$, $ghrl^{+/-}$, and $ghrl^{-/-}$ mice (data not shown). Measurement of ghrelin levels by ELISA indicated that the stomachs of $ghrl^{-/-}$ mice did not contain ghrelin. Immunohistochemistry also demonstrated the absence of ghrelin-producing cells in the stomachs of $ghrl^{-/-}$ mice (data not shown). We observed a normal birth ratio of $ghrl^{+/+}$, $ghrl^{+/-}$, and $ghrl^{-/-}$ mice as predicted by Mendelian genetics ($ghrl^{+/+}$: $ghrl^{+/-}$: $ghrl^{-/-}$ = 243 : 498 : 257). All

ghrl$^{-/-}$ mice appeared grossly normal, undergoing normal development to reach adulthood. Male *ghrl*$^{+/+}$, *ghrl*$^{+/-}$, and *ghrl*$^{-/-}$ mice had similar body weights at all ages (Fig. 1A).

3.2. Feeding pattern of *ghrl*$^{-/-}$ mice

We hypothesized that ghrelin plays a major role in promoting appetite and regulating feeding patterns. To test this hypothesis, we tested if genetic deletion of ghrelin decreased food intake. When *ghrl*$^{-/-}$ mice were fed standard chow, we did not observe any significant differences in the cumulative food intake over 10 weeks between male *ghrl*$^{-/-}$ and *ghrl*$^{+/+}$ littermates (Fig. 1B). In addition, there were no significant differences in feeding patterns between *ghrl*$^{+/+}$ and *ghrl*$^{-/-}$ littermates, despite measurement of food intake every 15 min over 11 days using the K2-CABIN apparatus (Fig. 2A). *Ghrl*$^{-/-}$ mice ate higher quantities of food in dark phase than in light phase, which was similar to *ghrl*$^{+/+}$ littermates (Fig. 2B). These results indicate that ghrelin does not have an essential role in feeding patterns.

3.3. Adaptation capability to negative energy states of *ghrl*$^{-/-}$ mice

If ghrelin is necessary for the feeding behaviors induced by negative energy state, *ghrl*$^{-/-}$ mice may exhibit abnormal behaviors during scheduled feeding. Within one week, *ghrl*$^{+/+}$ and *ghrl*$^{-/-}$ littermates both adapted to scheduled feedings, consuming the same amount of food per day (Fig. 3). There were also no differences in water intake or body weight between the

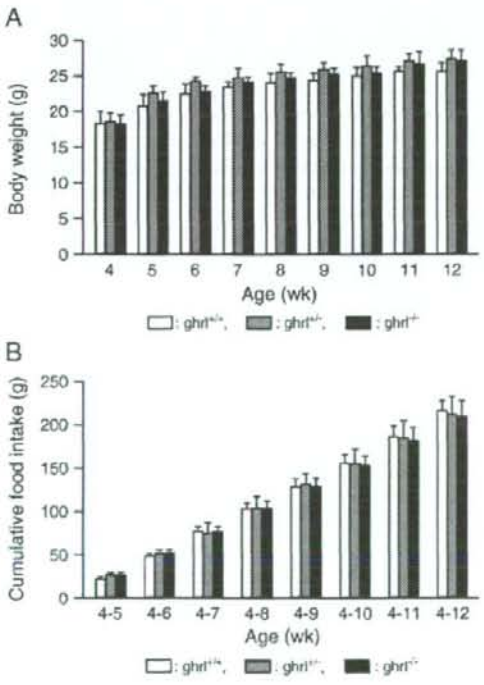

Fig. 1. *Ghrl*$^{-/-}$ mice exhibit normal growth rates and food intake. (A) Body weight; (B) cumulative food intake. Mice were four weeks old at the beginning of the study (n=8, P>0.05 [*ghrl*$^{+/+}$, *ghrl*$^{+/-}$ versus *ghrl*$^{-/-}$ mice]).

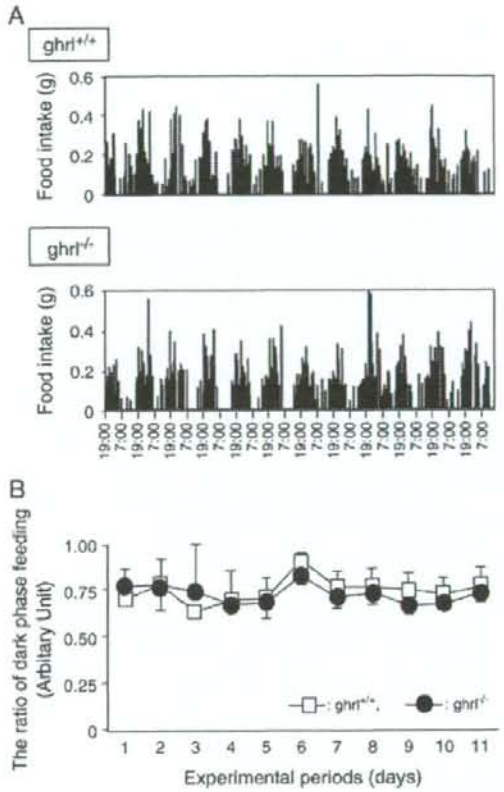

Fig. 2. *Ghrl*$^{-/-}$ mice display normal feeding patterns. (A) Food intake was recorded every 15 min for 11 days; (B) The ratio of dark phase feeding to total feeds (n=6, P>0.05 [*ghrl*$^{+/+}$ versus *ghrl*$^{-/-}$ mice]).

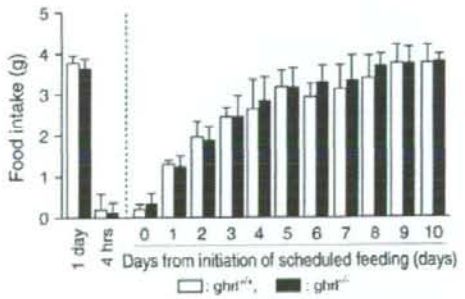

Fig. 3. The adaptation capability of *ghrl*$^{-/-}$ mice to a negative energy state is also normal (n=6, P>0.05 [*ghrl*$^{+/+}$ versus *ghrl*$^{-/-}$ mice]).

two groups (data not shown). These results demonstrate that *ghrl*$^{-/-}$ mice can adapt to a negative energy state.

3.4. Memory-related feeding performances of *ghrl*$^{-/-}$ mice

To test the physiologic role of ghrelin in feeding memory, we performed a food search test. Low values in *ghrl*$^{-/-}$ mice in comparison to *ghrl*$^{+/+}$ mice would indicate a critical role for ghrelin in this process. To test this assumption, we used a novel apparatus called KUROBOX. This apparatus has four food stations, named regions of interest (ROI), in the four corners of the cage (Fig. 4A). At any one time, however, the mouse can only take powder food from a single station. The correct food station rotated counter-clockwise every 4 h. To analyze the food searching behavior of mice, we used the correct visit ratio. This index is the ratio of visits to the correct ROI to the number of visits to all ROIs. In this experiment, the correct visit ratio was the same for *ghrl*$^{-/-}$ mice as that observed for *ghrl*$^{+/+}$ littermates; this index increased with time in both groups (Fig. 4B). Thus, *ghrl*$^{-/-}$ mice did not exhibit impaired feeding memory.

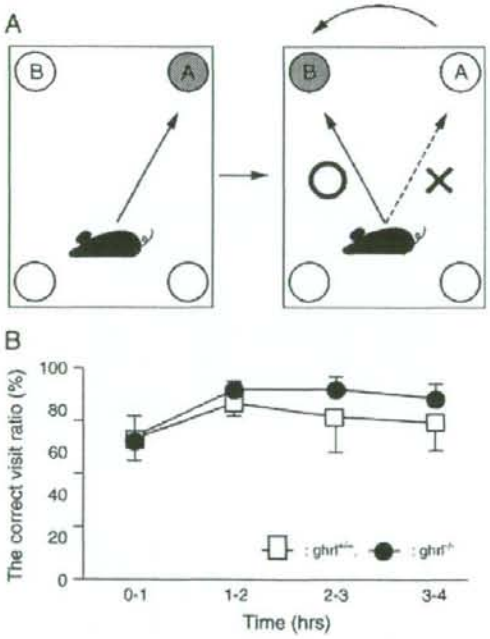

Fig. 4. The memory of feeding in *ghrl*$^{-/-}$ mice is normal. (A) Schematic illustration of the principles of KUROBOX analysis. When feed is first put in ROI A, the mouse always goes to ROI A to eat. Immediately after transferring feeds from ROI A to B, however, the mouse goes to ROI A by mistake at first. Gradually, the mouse goes to the correct ROI B. Investigation of the way of access can help estimate memory tasks in these mice. (B) The correct visit ratio is defined as the ratio of the number of visits to the correct food station to the number of visits to all stations ($n=6$, $P>0.05$ [*ghrl*$^{+/+}$ versus *ghrl*$^{-/-}$ mice]).

4. Discussion

Ghrelin has effects on puberty onset and pregnancy outcomes in rats [11]. Ghrelin also modulates rat testicular function and regulates gonadotropin secretion [12–14]. *Ghrl*$^{-/-}$ mice, however, were fertile and delivered normal litter sizes, indicating that ghrelin is not essential for reproductive function. While a number of reports indicate that ghrelin induces cell proliferation [15–17], there were no gross differences in tissue weights or body weights between *ghrl*$^{+/+}$ *and ghrl*$^{-/-}$ mice. There were no physical or tissue abnormalities identified in *ghrl*$^{-/-}$ mice by our routine analytical protocols. These results suggested that ghrelin is not critical for cell proliferation.

Centrally- or peripherally-injected ghrelin induces acute food intake in rats [18,19]. Ghrelin receptors localize in the SCN and the Arc, important regions in the regulation of circadian rhythms and feeding, respectively [4], suggesting that ghrelin maybe involved in feeding initiation and patterns. *Ghrl*$^{-/-}$ mice, however, have normal feeding patterns, with high food intake in dark phase and low intake in light phase. These results indicate that ghrelin is neither an initiator of feeding nor a regulator of feeding patterns. Ghrelin may act on the SCN to play an unknown role(s) in feeding patterns.

Fasting induces ghrelin secretion from the hypothalamus and stomach in rats [3]. Negative energy states induced by centrally-administered 2-deoxy-D-glucose also stimulates ghrelin secretion from the rat hypothalamus [3]. Plasma ghrelin levels are increased in anorexia nervosa patients and returns to basal levels following weight gain and recovery in these patients [20]. Patients with chronic heart failure (CHF) or chronic obstructive pulmonary disease (COPD) often exhibit a degree of cachexia. Plasma ghrelin levels were significantly higher in CHF patients with cachexia than those without cachexia [21]. Similarly, plasma ghrelin was elevated in underweight patients with COPD, in whom the levels were associated with a cachectic state [22]. Thus, ghrelin secretion is induced by negative energy states, suggesting that ghrelin is necessary for adaptation to negative energy states. In both *ghrl*$^{+/+}$ and *ghrl*$^{-/-}$ mice, however, the capacity to adapt to scheduled feeding was normal. Mice in both groups required approximately one week to eat the same amount of food during over one day. Thus, the absence of ghrelin does not physiologically change the scheduled feedings of mice.

Recently, ghrelin was shown to control hippocampal spine synapse density and memory performance [23]. Therefore, we investigated the memory-related feeding performance of *ghrl*$^{-/-}$ mice using the KUROBOX apparatus. This powerful tool allows us to analyze the memory of feeding. We could not, however, observe any differences in memory-related feeding performance between *ghrl*$^{+/+}$ and *ghrl*$^{-/-}$ mice. In both groups, the correct visit ratio increased with time after transfer of feedings. This result indicates that ghrelin does not control the food searching behaviors or the memory of feeding.

In summary, we did not observe any changes in the feeding performances of *ghrl*$^{-/-}$ mice in this study. Multiple previous reports have demonstrated that ghrelin has an important role in feeding regulation. Therefore, we cannot exclude the possibility that compensatory mechanisms may work to regulate feeding in

ghrl$^{-/-}$ mice. Although we also investigated the gene expression of a subset of orexigenic and anorexigenic peptides, we did not observe any differences between the two groups. It remains possible that an unknown mechanism regulates feeding. Thus, this study demonstrates that ghrelin is not critically required for feeding performance. Further studies will be needed to reveal the essential role(s) of ghrelin in these animals.

Acknowledgments

We thank Y. Yamashita and Y. Yoshida (Kurume University), and A. Kawai and Y. Maruyama (Osaka University) for their helpful assistance.

The studies in the authors' laboratory are supported by grants from Research on Measures for Intractable Diseases from the Health and Labour Sciences Research Grants, the MEXT Open Research Center Project (2004). And this work was supported in part by the Promotion of Basic Research Activities for Innovative Biosciences (PROBRAIN) (to M.K.), by Grant-in-Aids for Scientific Research from the Ministry of Education, Culture, Sports, Science and Technology of Japan (to M.K.), by Kato Memorial Bioscience Foundation (to T.S.), by The Foundation for Growth Science (to T.S.), and by the Sasakawa Scientific Research Grant (to T.S).

References

[1] Kojima M, Hosoda H, Date Y, Nakazato M, Matsuo H, Kangawa K. Ghrelin is a growth-hormone-releasing acylated peptide from stomach. Nature 1999;402:656–60.

[2] Dezaki K, Yada T. Ghrelin in the regulation of glucose and lipid metabolism. Nippon Rinsho 2004;62(Suppl 9):388–91.

[3] Sato T, Fukue Y, Teranishi H, Yoshida Y, Kojima M. Molecular forms of hypothalamic ghrelin and its regulation by fasting and 2-deoxy-D-glucose administration. Endocrinology 2005;146:2510–6.

[4] Zigman JM, Jones JE, Lee CE, Saper CB, Elmquist JK. Expression of ghrelin receptor mRNA in the rat and the mouse brain. J Comp Neurol 2006;494:528–48.

[5] Kamegai J, Tamura H, Shimizu T, Ishii S, Sugihara H, Wakabayashi I. Chronic central infusion of ghrelin increases hypothalamic neuropeptide Y and agouti-related protein mRNA levels and body weight in rats. Diabetes 2001;50:2438–43.

[6] Goto M, Arima H, Watanabe M, Hayashi M, Banno R, Sato I, et al. Ghrelin increases neuropeptide Y and agouti-related peptide gene expression in the arcuate nucleus in rat hypothalamic organotypic cultures. Endocrinology 2006;147:5102–9.

[7] Toshinai K, Date Y, Murakami N, Shimada M, Mondal MS, Shimbara T, et al. Ghrelin-induced food intake is mediated via the orexin pathway. Endocrinology 2003;144:1506–12.

[8] Cowley MA, Cone RD, Enriori P, Louiselle I, Williams SM, Evans AE. Electrophysiological actions of peripheral hormones on melanocortin neurons. Ann N Y Acad Sci 2003;994:175–86.

[9] Sato T, Yamaguchi T, Matsuzaki M, Satoh T, Suzuki A. Mammosomatotrophs develop within mammotroph clusters in bovine adenohypophysis. Tissue Cell 1999;31:499–504.

[10] Kurokawa M, Fujimura K, Sakurai-Yamashita Y. A new-generation apparatus for studying memory-related performance in mice. Cell Mol Neurobiol 2003;23:121–9.

[11] Fernandez-Fernandez R, Navarro VM, Barreiro ML, Vigo EM, Tovar S, Sirotkin AV, et al. Effects of chronic hyperghrelinemia on puberty onset and pregnancy outcome in the rat. Endocrinology 2005;146:3018–25.

[12] Furuta M, Funabashi T, Kimura F. Intracerebroventricular administration of ghrelin rapidly suppresses pulsatile luteinizing hormone secretion in ovariectomized rats. Biochem Biophys Res Commun 2001;288:780–5.

[13] Tena-Sempere M. Ghrelin: novel regulator of gonadal function. J Endocrinol Invest 2005;28:26–9.

[14] Tena-Sempere M, Barreiro ML, Gonzalez LC, Gaytan F, Zhang FP, Caminos JE, et al. Novel expression and functional role of ghrelin in rat testis. Endocrinology 2002;143:717–25.

[15] Kim SW, Her SJ, Park SJ, Kim D, Park KS, Lee HK, et al. Ghrelin stimulates proliferation and differentiation and inhibits apoptosis in osteoblastic MC3T3-E1 cells. Bone 2005;37:359–69.

[16] Nanzer AM, Khalaf S, Mozid AM, Fowkes RC, Patel MV, Burrin JM, et al. Ghrelin exerts a proliferative effect on a rat pituitary somatotroph cell line via the mitogen-activated protein kinase pathway. Eur J Endocrinol 2004;151:233–40.

[17] Duxbury MS, Waseem T, Ito H, Robinson MK, Zinner MJ, Ashley SW, et al. Ghrelin promotes pancreatic adenocarcinoma cellular proliferation and invasiveness. Biochem Biophys Res Commun 2003;309:464–8.

[18] Nakazato M, Murakami N, Date Y, Kojima M, Matsuo H, Kangawa K, et al. A role for ghrelin in the central regulation of feeding. Nature 2001;409:194–8.

[19] Date Y, Murakami N, Toshinai K, Matsukura S, Niijima A, Matsuo H, et al. The role of the gastric afferent vagal nerve in ghrelin-induced feeding and growth hormone secretion in rats. Gastroenterology 2002;123:1120–8.

[20] Cuntz U, Fruhauf E, Wawarta R, Tschop M, Folwaczny C, Riepl R, et al. A role for the novel weight-regulating hormone ghrelin in anorexia nervosa. Am Clin Lab 2002;21:22–3.

[21] Nagaya N, Uematsu M, Kojima M, Date Y, Nakazato M, Okumura H, et al. Elevated circulating level of ghrelin in cachexia associated with chronic heart failure: relationships between ghrelin and anabolic/catabolic factors. Circulation 2001;104:2034–8.

[22] Itoh T, Nagaya N, Yoshikawa M, Fukuoka A, Takenaka H, Shimizu Y, et al. Elevated plasma ghrelin level in underweight patients with chronic obstructive pulmonary disease. Am J Respir Crit Care Med 2004;170:879–8782.

[23] Diano S, Farr SA, Benoit SC, McNay EC, da Silva I, Horvath B, et al. Ghrelin controls hippocampal spine synapse density and memory performance. Nat Neurosci 2006;9:381–8.

THE JOURNAL OF BIOLOGICAL CHEMISTRY VOL. 282, NO. 42, pp. 30373–30380, October 19, 2007
© 2007 by The American Society for Biochemistry and Molecular Biology, Inc. Printed in the U.S.A.

PGAP1 Knock-out Mice Show Otocephaly and Male Infertility*

Received for publication, July 9, 2007, and in revised form, August 15, 2007 Published, JBC Papers in Press, August 20, 2007, DOI 10.1074/jbc.M705601200

Yasutaka Ueda[‡], Ryo Yamaguchi[§], Masahito Ikawa[§], Masaru Okabe[§], Eiichi Morii[¶], Yusuke Maeda[‡], and Taroh Kinoshita[‡1]

From the [‡]Department of Immunoregulation and the [§]Genome Information Research Center, Research Institute for Microbial Diseases, Osaka University, 3-1 Yamada-oka, Suita, Osaka 565-0871 and the [¶]Department of Pathology, Osaka University Medical School, Yamada-oka 2-2, Suita, Osaka 565-0871, Japan

A palmitate linked to the inositol in glycosylphosphatidylinositol (GPI) is removed in the endoplasmic reticulum immediately after the conjugation of GPI with proteins in most cells. Previously, we identified PGAP1 (post GPI attachment to proteins 1) as a GPI inositoldeacylase that removes the palmitate from inositol. A defect in PGAP1 caused a delay in the transport of GPI-anchored proteins (GPI-APs) from the endoplasmic reticulum to the cell surface in Chinese hamster ovary cells, although the cell-surface expression of GPI-APs in the steady state was normal. Nevertheless, in most cells, GPI-APs undergo deacylation. To elucidate the biological significance of PGAP1 *in vivo*, we established PGAP1 knock-out mice. Most PGAP1 knock-out mice showed otocephaly, a developmental defect, and died right after birth. However, some survived with growth retardation. Male knock-out mice showed severely reduced fertility despite the capability of ejaculation. Their spermatozoa were normal in number, motility, and ability to ascend the uterus, but were unable to go into the oviduct. *In vitro*, PGAP1-deficient spermatozoa showed weak attachment to the zona pellucida and a severely diminished rate of fertilization. Therefore, an extra acyl chain in GPI anchors caused severe deleterious effects to development and sperm function.

Many eukaryotic cell-surface proteins with various functions are anchored to the membrane via glycosylphosphatidylinositol (GPI)[2] (1–3). The structure of GPI is well conserved among eukaryotes. More than 150 GPI-anchored proteins (GPI-APs) with various functions have been identified, including complement system regulatory factors (CD55 and CD59), enzymes (acetylcholinesterase, alkaline phosphatase, and others), adhesion molecules (CD48, neural cell adhesion molecule, and others), and receptors for signal transduction (lipopolysaccharide receptor, urokinase-type plasminogen activator receptor, folate receptor, and others) (3, 4). The GPI anchor is synthesized in the endoplasmic reticulum (ER), consisting of ethanolamine phosphate, three mannoses, glucosamine, and phosphatidylinositol (3, 5, 6), and is transferred to proteins. Phosphatidylinositol glycan A is the enzyme involved in the early step of GPI synthesis, and its disruption in mice causes complete loss of GPI synthesis resulting in embryonic lethality with defective gastrulation and neural development indicating the importance of GPI-APs for normal development (7).

At an early step, the inositol ring of GPI is acylated with a palmitoyl chain by phosphatidylinositol glycan W (8). This inositol acylation is indispensable for the attachment of ethanolamine phosphate to the third mannose of GPI intermediates, and phosphatidylinositol glycan W-defective mutant cells express very low levels of GPI-APs (8). Soon after the attachment of mature GPI to proteins, the inositol is usually deacylated in the ER (9). This process is necessary for efficient transport of GPI-APs to the plasma membrane by vesicular trafficking (10). GPI-APs accumulate in specific microdomains in the plasma membrane called lipid rafts, which are enriched in sphingolipids and cholesterol (11–13). GPI-APs are incorporated into lipid rafts in the Golgi and transported to the cell surface (11). Rafts are the portals for endocytosis and the platforms for signal transduction and mediate apical sorting of GPI-APs (12–15). Previously, we established mutant cells based on resistance to bacterial PI-PLC, which cleaves GPI-APs unless palmitoylated on the inositol (16–18), and identified PGAP1 as the inositoldeacylase (10). A clear delay in the glycosylation of GPI-APs was observed, and the accumulation of ER-form GPI-APs was obvious, indicating the transport of GPI-APs from ER to Golgi was delayed; however, cell-surface expression of GPI-APs was not affected (10). On most cells, except human erythrocytes, GPI-APs are deacylated (16–18). Why should most GPI-APs on the membrane be deacylated? To clarify the physiological role of this deacylation, we generated PGAP1 knock-out mice.

EXPERIMENTAL PROCEDURES

Generation of PGAP1-deficient Mice—The targeting vector for deletion of *PGAP1* exon 5 contains an expression cassette of the neomycin resistance gene (neo) for positive selection and diphtheria toxin for negative selection. The target vector was linearized by digestion with Asc-I and electroporated into mouse D3 embryonic stem cells. Homologous recombinants were selected using G418, PCR, and Southern blotting and were injected into C57BL/6 mouse blastocysts. PCR for the first embryonic stem cell screening was performed using primer1 (5′-TAgCCTggAggACAACAgAT-

* This work was supported by grants from the Ministry of Education, Culture, Sports, Science, and Technology of Japan and the Core Research for Evolutional Science and Technology, Japan Science and Technology Agency. The costs of publication of this article were defrayed in part by the payment of page charges. This article must therefore be hereby marked "*advertisement*" in accordance with 18 U.S.C. Section 1734 solely to indicate this fact.

[1] To whom correspondence should be addressed. Tel.: 81-6-6879-8328; Fax: 81-6-6875-5233; E-mail: tkinoshi@biken.osaka-u.ac.jp.

[2] The abbreviations used are: GPI, glycosylphosphatidylinositol; PGAP1, post GPI attachment to proteins 1; GPI-APs, GPI-anchored proteins; ER, endoplasmic reticulum; PI-PLC, phosphatidylinositol-specific phospholipase C; ZP, zona pellucida; ADAM, a disintegrin and metalloprotease; ACE, angiotensin-converting enzyme; tACE, testis-specific ACE; DAF, decay-accelerating factor; Dally, division abnormally delayed; Dlp, Dally-like proteins; PBS, phosphate-buffered saline; WT, wild type; KO, knock-out; E, embryonic day.

Downloaded from www.jbc.org at Keio University Shinanomachi Media Center on March 6, 2008

ACTCAT-3') and primer2 (5'-gTTATTCggTCCCTCgAATAgg-TTCA-3'). Chimeric male mice were crossed with C57BL/6 J female mice (CLEA Japan, Inc., Tokyo) to establish heterozygous mutant lines. Genotyping was performed with the pair of primer3 (5'-TCCATgCAgTgTTTggCTgTAAgTC-3') and primer4 (5'-TAgCAAAgATAAACCATAggAgCACCC-3') for wild type, generating a 355-bp band, and the pair of primer3 and primer5 (5'-gTTATTAggTCCCTCgAAgAggTTCA-3') for knock-out mice, generating a 269-kb band. Homozygous knock-out mice were obtained by crossing heterozygous male with female mice. All animal experiments were carried out according to the Guide for the Care and Use of Laboratory Animals in Osaka University.

Southern Blotting—Genomic DNA was prepared from the tail, digested with BspHI or NdeI, and separated by agarose gel electrophoresis. The probe B was generated by PCR using the set of primer A (5'-gAggCgCgCCAAgAAgTAggggTgTAgAgg-TTggT-3') and primer B (5'-gTTTATgATgAgTATCTgTTgT-CCTC-3'), and the probe N was generated by PCR using the set of primer C (5'-ACTggAACACTTTTgTgACATgggAA-3') and primer D (5'-ATAAggCACTggTgTAATggCTCAAT-3').

PI-PLC Assay—White blood cells derived from 300 μl of peripheral blood were diluted with 100 μl of Dulbecco's modified Eagle's medium containing 1 unit/ml PI-PLC (Molecular Probes) and 0.02 M HEPES buffer (Sigma). Samples were incubated at 37 °C for 30 min, and the cells were subjected to fluorescence-activated cell sorting analysis. The antibodies used were allophycocyanin-conjugated anti-mouse CD4 (RM4–5), fluorescein isothiocyanate-conjugated anti-mouse CD8α(Ly-2), fluorescein isothiocyanate-conjugated anti-mouse CD45R/B220 (RA3–6B2), allophycocyanin-conjugated anti-mouse T cell receptor β chain (H57–597) and phycoerythrin-conjugated Armenian hamster anti-mouse CD48 (BCM1, HM48-1, IgG1, and lamda3, all from BD Pharmingen). Phycoerythrin-conjugated Armenian hamster IgG1, lamda1 (anti-TNP, BD Pharmingen) was used as an isotype control for the phycoerythrin-conjugated Armenian hamster anti-mouse CD48. Data obtained by FACSCalibur (BD Biosciences) were analyzed with FlowJo (TreeStar, Inc.).

In Vivo Mating—Each experimental and control mouse was mated with 3 female BDF-1 mice for 8 weeks. The females were allowed to deliver the pups, which were counted after birth. The females that failed to become pregnant when mated with PGAP1$^{-/-}$ mice were later tested for fertility by mating with normal males.

Sperm Migration Assay—Ascent of sperm from the uterus into oviduct was examined as described previously (19). B6DF1 female mice at 8 weeks of age were superovulated by intraperitoneal injection of 5 units of pregnant mare's serum gonadotropin (Teikoku Zoki Co., Tokyo), followed by injection of 5 units of human chorionic gonadotropin (Teikoku Zoki Co.) 48 h later. Superovulated females were mated with PGAP1 mutant males of each genotype 12 h after human chorionic gonadotropin injection, and the formation of a vaginal plug was observed every 30 min. About 2 h after copulation, oviducts were excised with the connective part of the uterus, fixed in PBS containing 4% paraformaldehyde for 6 h at 4 °C, washed with PBS, and frozen in OCT compound (Sakura Finetechnical Co., Tokyo) with liquid nitrogen. Sections were prepared, stained with hematoxylin, and then observed under a microscope.

In Vitro Fertilization—The capacitation was induced *in vitro* by incubating sperm from PGAP1 homozygous mutant and wild-type littermates in TYH medium (modified Krebs-Ringer bicarbonate solution containing glucose, sodium pyruvate, bovine serum albumin, and antibiotics) (20). Ovulated egg masses from B6DF1 mice (>2 months old, Japan SLC, Inc., Shizuoka, Japan) were placed in a 200-μl drop of TYH medium. An aliquot of capacitated sperm (2×10^5 sperm/ml) was inseminated. The mixture was incubated for 8 h at 37 °C under 5% CO_2 in air (21). Approximately 60–80 eggs for each genotype were examined for fertility by pronuclei formation. For the sperm-zona binding assay, egg masses were treated with bovine testicular hyaluronidase (175 units/ml, Sigma) for 5 min to remove the cumulus cells. Cumulus-free eggs were placed in a 200-μl TYH drop and inseminated. After 30 min of incubation, sperm bound to the zona pellucida of the eggs were observed using an IX-70 microscope (Olympus). We did not differentiate the state of sperm on the zona pellucida, "attaching" and "binding," so the eggs were observed without washing by pipetting.

Antibodies—Affinity-purified rabbit anti-SPAM1 (PH-20) antibody was a kind gift from Dr. Tadashi Baba (University of Tsukuba, Ibaraki, Japan) (22). Monoclonal antibodies against mouse ADAM2 (9D2.2) and ADAM3 (7C1.2) were purchased from Chemicon International, Inc. Monoclonal antibody against tACE (1D5) was prepared as described (23). An Armenian hamster monoclonal antibody against mouse GPI-DAF (RIKO-4) was a kind gift from Drs. Hidechika Okada and Noriko Okada (Nagoya City University, Nagoya, Japan) (24). A polyclonal antibody against Izumo was prepared as described (25). An antibody against CD59b was a kind gift from Dr. B. Paul Morgan (University of Wales College of Medicine, UK) (26).

Preparation of Protein Extracts—Mice testes were washed with cold PBS, and their covering tunica albuginea were removed in cold PBS. Testicular tubes were further washed in PBS and homogenized in 25 volumes of lysis buffer (20 mM Tris-HCl, pH 7.4, 1% Triton X-100, 150 mM NaCl, 10 μg/ml aprotinin, 10 μg/ml leupeptin, 1 mM phenylmethylsulfonyl fluoride) using a Micro Multi Mixer (IEDA Trading Corp., Tokyo). The protein concentrations of homogenates of each sample were measured using a BCA™ Protein Assay Kit (Pierce) and adjusted appropriately.

Mouse sperm were collected from the cauda epididymis and vas deferens, washed with 4 °C PBS once, and centrifuged at 810 × *g* for 3 min at 4 °C. The pellet was lysed with the same lysis buffer, and the protein concentration was adjusted in the same manner as testes.

Western Blotting—Protein extracts were centrifuged at 15,000 × *g* for 10 min at 4 °C to remove the insoluble protein and debris, and the supernatants were colleted. Proteins were separated by SDS-PAGE under reducing conditions (ADAM2, ADAM3, tACE, and Izumo) or non-reducing conditions (CD55, CD59b, SPAM-1, CD52) and transferred electrophoretically to polyvinylidene difluoride membranes. After blocking with TBS-T buffer (20 mM Tris-HCl (pH7.4), 150 mM NaCl, 0.05% Tween 20) containing 5% skim milk overnight, blots were incubated with primary antibodies for 1 h at room temperature. Membranes were

Downloaded from www.jbc.org at Keio University Shinanomachi Media Center on March 6, 2008

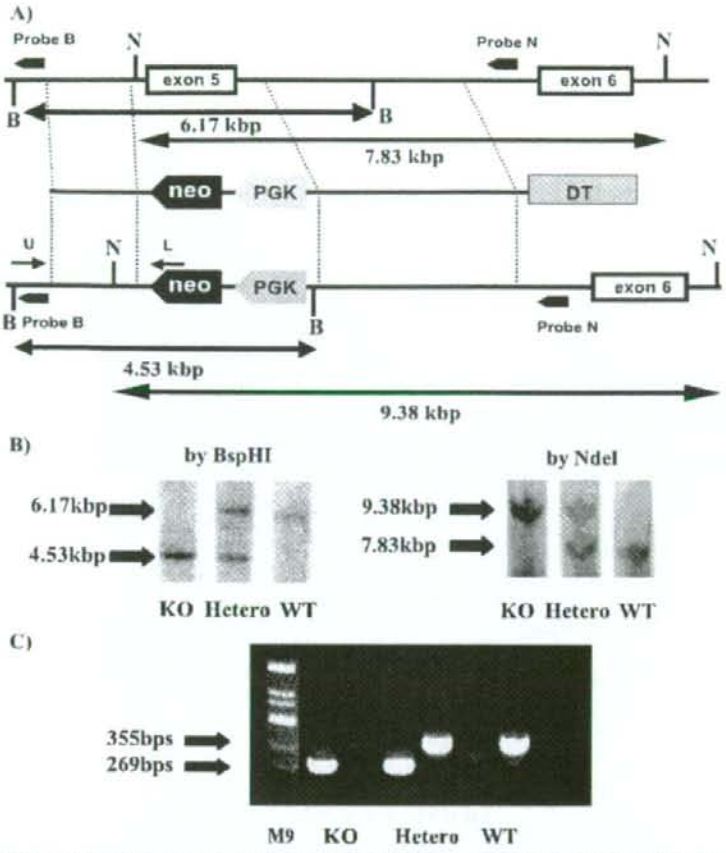

FIGURE 1. In *A*, the *top diagram* is a schematic representation of the normal PGAP1 allele; the *middle diagram* shows the targeting construct with PGK neomycin (neo) as a positive selectable marker and diphtheria toxin (*DT*) as a negative selective marker. This construct was designed to delete the PGAP1 gene. The *bottom diagram* shows the PGAP1 allele mutated by homologous recombination. The exons are represented by *blank boxes*. PCR primers for homologous recombination screening are represented by the *short arrows* labeled *U* and *L*. *B*, genotyping by Southern blot analysis of DNA purified from the tails of F2 mice generated from crossing with PGAP1$^{+/-}$ F1 pups. After cutting with the restriction enzymes BspHI (for the upstream part) or NdeI (for the downstream part), DNA was hybridized with non-radioisotope-labeled probes shown as *Probe B* (for the upstream part) or *Probe N* (for the downstream part). The *bold "B"* or *"N"* in *panel A* shows restriction sites for BspHI or NdeI. *C*, genotyping by PCR was performed using three kinds of primers. PGAP1 (−/−) was detected as a single band at 269 bp using the pair of primer3 and primer5, PGAP1 (+/+) was detected at 355 bp using the pair of primer3 and primer4, and PGAP1 (+/−) mice express both bands.

then washed with TBS-T buffer twice and incubated with the appropriate second antibodies. Detection of bands was performed using a Western Lightning™ kit (PerkinElmer Life Sciences). Signal intensities were determined using the Fujifilm LAS-1000 system (Fuji Photo Film Co., Ltd., Japan). Triton X-114-mediated partitioning of proteins into aqueous and detergent phases was done as described (10).

Statistical Analysis—All the statistical analyses were done with JMP Start Statistics (SAS Institute Inc.).

RESULTS

Generating PGAP1 Knock-out Mice—The targeting construct for generating PGAP1 knock-out mice was designed to delete exon 5 of the PGAP1 gene, which contains a serine-containing catalytic motif (10). Five chimeric male mice were able to sire PGAP1$^{+/-}$ mice. The analyses of PGAP1 knock-out mouse in this report are basically based on the first PGAP1$^{-/-}$ line, and the phenotypes observed in the first line were also examined in other lines derived from different embryonic stem cells. The genotypes of wild-type (PGAP1$^{+/+}$), heterozygous (PGAP1$^{+/-}$), and homozygous mutant (PGAP1$^{-/-}$) mice were identified by PCR and Southern blot analyses of genomic DNA (Fig. 1). Peripheral blood cells of each genotype were tested for PI-PLC resistance. CD48, a GPI-AP, on wild-type but not knock-out TCR-β-positive mononuclear cells was sensitive to PI-PLC (Fig. 2). The same result was observed with B220-positive mononuclear cells (data not shown), indicating that PGAP1 was successfully knocked out in homozygous mutants.

High Frequency of Perinatal Death and Otocephaly of PGAP1 Knock-out Mice—Breeding of PGAP1$^{+/-}$ male and female mice resulted in a smaller number of homozygous mutant mice than expected from Mendelian genetics (PGAP1$^{+/+}$:PGAP1$^{+/-}$:PGAP1$^{-/-}$ = 55(26%):122(57%):36(17%)). Most PGAP1$^{-/-}$ (31 out of 36 pups) died right after delivery or within 24 h of birth. More than half of the dead homozygous mutant mice showed severely disturbed face and jaw shaping, which seemed similar to the phenotype of otocephaly in mammalian species and humans (27–30) (Fig. 3). The severity of otocephaly varied among the knock-out mice from a normal face to a complete lack of mouth and jaw. Even the most affected were alive on delivery but soon became cyanotic and died. PGAP1 knock-out mice with normal faces were active and vigorous after birth, but milk was not observed in their stomachs when they died, even though behaviors of heterozygous mothers (retrieval and licking the pups) were observed. Those who survived the critical 24 h after birth were able to survive like other littermates, and finally we obtained four male and one female adult homozygous knock-out mice. The number of PGAP1$^{-/-}$ mice, even including dead ones, was smaller than that of expected from Mendelian genetics. To examine the possibility of embryonic lethality, we performed cesarean operations on pregnant mice at 18.5 days post coitus. Genotypes of 30 embryos from 3 mice were PGAP1$^{+/+}$:

Downloaded from www.jbc.org at Keio University Shinanomachi Media Center on March 6, 2008

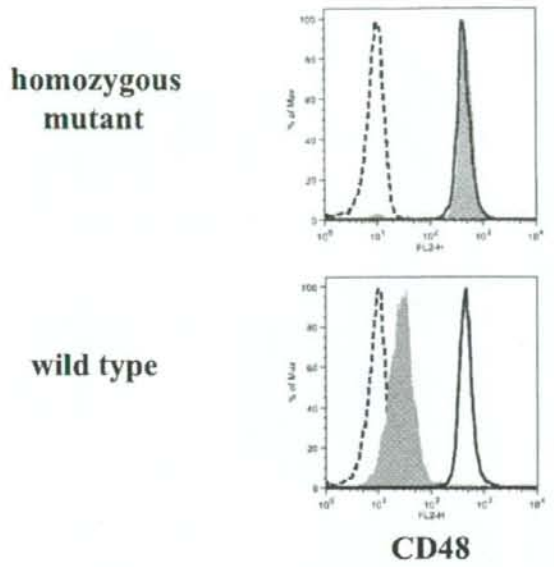

FIGURE 2. **PI-PLC resistance of peripheral blood of each genotype.** Peripheral blood of knock-out or wild-type mouse was treated with (+) or without (−) PI-PLC for 30 min at 37 °C, and the surface expression of CD48 was analyzed by fluorescence-activated cell sorting. The *dotted line* shows the staining obtained with an isotype control for the anti-CD48 antibody.

$PGAP1^{+/-}$:$PGAP1^{-/-}$ = 5:18:7. Four out of seven homozygous mutant mice showed otocephaly, but all of them were still alive in the amnia, suggesting that pups die immediately after birth. A comparison of sections from pups of each genotype showed that the brains of most homozygous mutants were degenerated, but that other organs looked intact. Most of the $PGAP1^{-/-}$ embryos lacked rostral structures. In $PGAP1^{-/-}$, the oropharynx and mandible were developed, but the size of the mandible was small. In severely affected ones, no maxillary bone, nasal cavity, nasal sinus, or olfactory bulb was observed. Although the formation of telencephalon was detected in both $PGAP1^{+/+}$ and $PGAP1^{-/-}$ embryos, the layer structure of $PGAP1^{-/-}$ embryos was immature. The cerebral cortex of $PGAP1^{+/+}$ embryos consisted of layers arranged parallel to the meningeal surface. The density and number of cells in the most superficial layer of $PGAP1^{-/-}$ mice was lower than that in $PGAP1^{+/+}$ mice, indicating an immature structure (Fig. 3). 43 embryos at 17.5–18.5 days post coitus derived from another embryonic stem clone had genotypes $PGAP1^{+/+}$:$PGAP1^{+/-}$:$PGAP1^{-/-}$ = 13:17:13. Three of the thirteen homozygous mutant mice showed severe otocephaly, two showed smaller faces, but all of the homozygous mutant pups were alive in the amnia.

PGAP1 Knock-out Mice Show Growth Retardation—Peripheral blood of each genotype was used in serological tests for liver function, kidney function, and other biochemical tests, but no clear deviation was observed among the genotypes. Blood cell counts and isotype deviation of CD4+/8+ cells in T cells, or B/T cells in lymphocytes, were also similar (data not shown). General screening for behavioral phenotyping was also performed. There was no significant difference between $PGAP1^{+/+}$ and $PGAP1^{-/-}$ mice with respect to general appearance, posture, gait, spontaneous behaviors, neurological reflexes, eyesight, and olfaction, but $PGAP1^{-/-}$ mice showed growth retardation compared with heterozygous or wild-type mutants, even though weaning and other dietary behavior looked normal (Fig. 4). Retarded growth curves were also observed in $PGAP1^{-/-}$ mutants in another clone (data not shown).

Male Infertility of PGAP1 Knock-out Mice—To analyze male fertility, 6 male homozygous mutant mice were mated each with 3 BDF-1 female mice for 8 weeks. Sibling $PGAP1^{+/-}$ or $PGAP1^{+/+}$ mice showed normal fertility, but none of the 6 $PGAP1^{-/-}$ mice sired a pup despite the presence of vaginal plugs after copulation, clearly indicating male infertility. One male homozygous mutant of another clone underwent the same experiment, and there was only one siring of 4 pups in 2-month mating, although plugs were admitted for each female wild-type mouse mated at least once during the period. Sibling $PGAP1^{+/-}$ or $PGAP1^{+/+}$ male mouse sired averages of 9.0 or 9.8 pups (total 54 and 49 pups each).

Knock-out Sperm Cannot Ascend from the Uterus into the Oviduct—Spermatozoa from $PGAP1^{-/-}$ mice were normal in number and motility (data not shown). Mammalian fertilization consists of multiple successive events, including sperm ascent from the uterus into the oviductal tube, sperm adhesion to the zona-pellucida (ZP), formation of a glycoprotein extracellular matrix surrounding the eggs, and membrane fusion of sperm and eggs. To examine at which step normal fertility is disturbed, firstly, we performed a sperm migration assay. Male mice of each genotype were mated with superovulated female wild-type mice. About 2 h after copulation, oviducts were excised with the connective part of the uterus, fixed, and stained to examine the presence of sperm in the oviductal tubes. Sperm from wild-type or heterozygous mutant mice were able to ascend into the oviduct, but those of homozygous mutant mice could not migrate into the oviductal tube (Fig. 5).

PGAP1 Knock-out Sperm Scarcely Bind to the ZP—To examine the ability of mutant sperm to bind to the ZP, we incubated sperm of wild-type or homozygous mutants with eggs in buffer and counted the number of sperm attached to the ZP. Homozygous mutant sperm showed poor binding to the ZP compared with wild-type sperm (WT:KO = 11.9:2.9 sperm per egg, $t < 0.0001$, unpaired Student's t test) (Fig. 6). The fertilization rate was examined with two pairs of WT and KO mice as

The Journal of Biological Chemistry

Downloaded from www.jbc.org at Keio University Shinanomachi Media Center on March 6, 2008

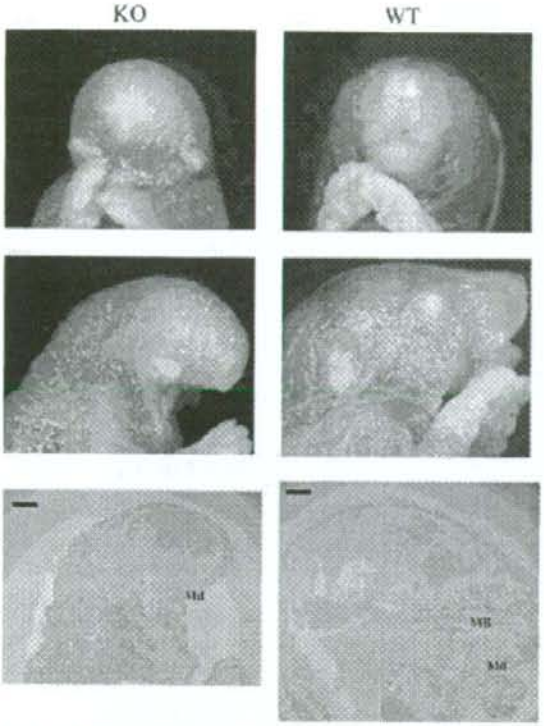

FIGURE 3. **PGAP1 knock-out mice showed otocephaly.** Pups at 20 days post coitus were fixed in PBS containing 4% paraformaldehyde. Severe otocephaly view of WT (*upper left panel*) or KO (*upper right panel*) sperm binding to the ZP. Each *lower panel* shows a magnified view of WT or KO sperm. Sections of WT and KO mice were stained with hematoxylin and eosin. KO mouse lacked the rostral part of the head (*lower left panel*). The oropharynx and mandible (*Md*) were developed, but the maxillary bone (*MB*) seen in WT mouse (*lower right panel*) was not observed in KO mouse (*lower left panel*). The formation of the telencephalon was detected in KO mouse, but the layer structure was immature as compared with WT mouse. *Bars* in the *boxes* represent 1 mm.

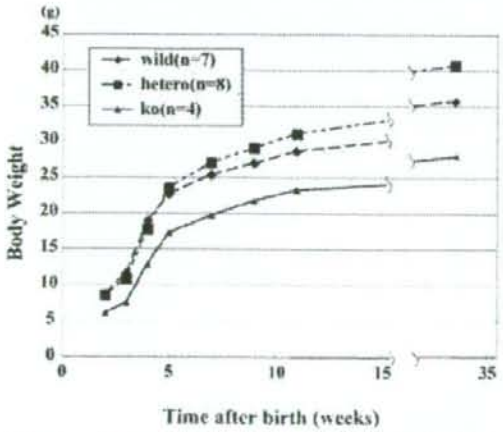

FIGURE 4. **Growth comparison of each genotype of male mice.** The body weight (g) of each genotype pup was measured at the weeks indicated. The *p* values for comparisons between wild-type and knock-out mice are 0.0055 at 4 weeks, 0.0175 at 11 weeks, and 0.0132 at 33 weeks.

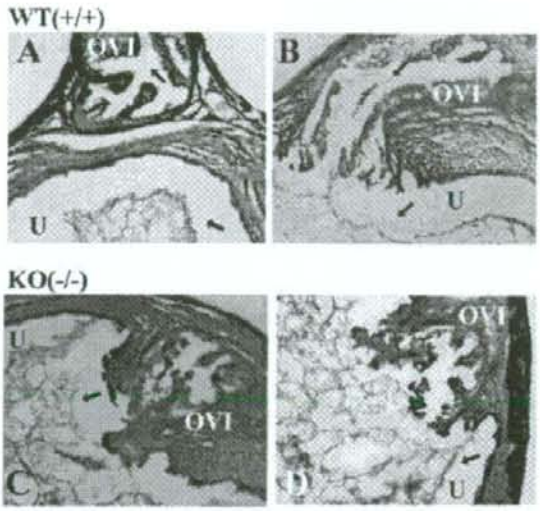

FIGURE 5. **Absence of migration of knock-out sperm into the oviduct.** The ascent of sperm from the uterus into the oviduct was examined in hematoxylin and eosin-stained frozen sections of the uterotubal junction 2 h after copulation. *A* and *B*, wild type; *C* and *D*, knock-out mice. *Arrows* represent sperm. In KO oviducts, no sperm was observed. *OVI*, oviduct; *U*, uterine lumen.

described under "Experimental Procedures": the average rate in the knock-out was 2.7% compared with 51.3% for wild-type sperm. Fusion of the sperm and egg was assessed by a zona-free egg sperm penetration assay (21), and both wild-type and homozygous mutant sperm showed normal fusion (data not shown). Poor sperm binding of knock-out mice was repeated in another PGAP1 knock-out line (WT:KO = 12.2:0.1 sperm per egg, $t < 0.0001$). In the second PGAP1 knock-out mouse line, the average fertilization rate was 27.2% for PGAP1$^{-/-}$ and 82.7% for wild type. In the second experiment, we used the mutant line crossed with AKR mice. A higher rate of fertilization *in vitro* with homozygous mutants may be due to the difference of genetic background or technical effects. These results indicate that PGAP1 knock-out male mice are infertile because of the inability of their sperm to ascend into the oviduct and bind the ZP.

Increased Expression Levels of GPI-APs in PGAP1$^{-/-}$ Mice—Next, we examined the expression in sperm of certain proteins that are presumably closely associated with sperm binding to the ZP, and with sperm migration from the uterus into the oviduct. Knock-out of calmegin (19, 31), ADAM1a (fertilin α) (32), ADAM2 (fertilin β) (33), ADAM3 (cyritestin) (34, 35), and testis-specific ACE (tACE) (36, 37) is reported to result in poor binding of sperm to the ZP. The sperm of calmegin knock-out mice are defective in the expression of ADAM2 and ADAM3 (19, 23), and homozygous ADAM1a mutant mice have ADAM3-deficient sperm. Therefore, we examined the expression of ADAM2, ADAM3, and tACE in testis and sperm. There was no significant reduction of ADAM2, ADAM3, and tACE in testis and sperm (Fig. 7*A*). Izumo is known as a protein that is indispensable for sperm-egg fusion (25), and its expression in knock-out mice was comparable to that in wild-type mice, consistent with the result that sperm-egg fusion was normal with

Downloaded from www.jbc.org at Keio University Shinanomachi Media Center on March 6, 2008

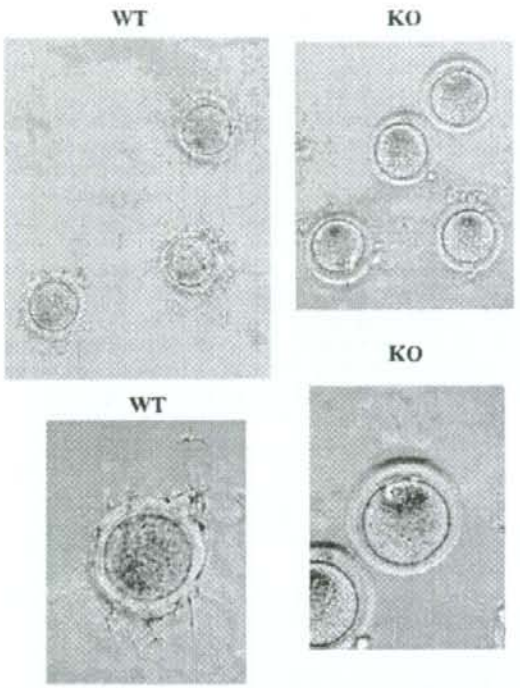

FIGURE 6. **Defective binding of PGAP1$^{-/-}$ sperm to the egg ZP.** Hyaluronidase-treated eggs were incubated with sperm of each genotype. Microscopic was detected in PGAP1$^{-/-}$ (KO) mice (*upper* and *middle left panels*) as compared with PGAP1$^{+/+}$ (WT) mice (*upper* and *middle right panels*).

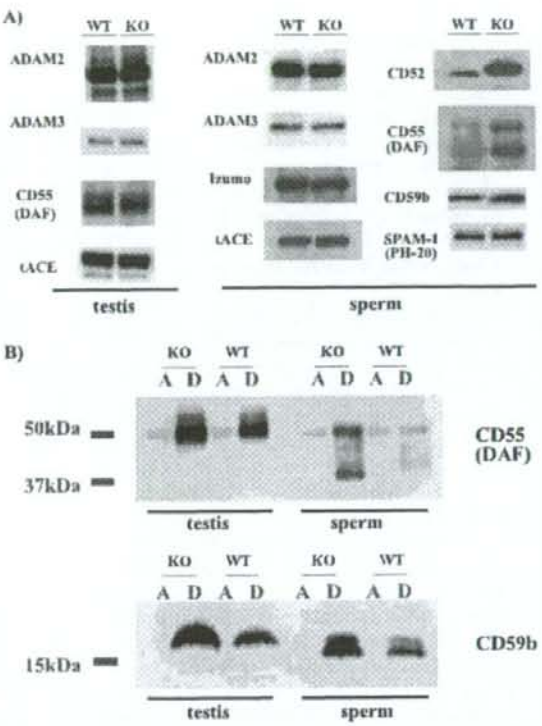

FIGURE 7. *A*, expression of proteins in mice of each genotype. Proteins from PGAP1 KO mice and WT mice were subjected to immunoblot analysis. Testicular proteins from mice of each genotype were subjected to immunoblotting using antibodies against ADAM2, ADAM3, CD55, and tACE (*left panels*). Spermatic proteins from mice of each genotype were subjected to immunoblotting using antibodies against ADAM2, ADAM3, Izumo, tACE, CD52, CD55, CD59b, and SPAM-1 (PH-20) (*right panels*). *B*, hydrophobicity of DAF and CD59b assessed by Triton X-114 partitioning. Protein samples were partitioned into aqueous (*A*) and detergent (*D*) phases before being subjected to immunoblot analysis as in *panel A*. *Top*, DAF; *bottom*, CD59b.

knock-out sperm. Notably, the amounts of GPI-APs in sperm were affected to various extents, in contrast to that of DAF in testis, which was normal (Fig. 7*A*). The amounts of both CD52 and DAF were significantly increased in knock-out mice, whereas CD59b and SPAM-1 (PH-20) were reproducibly increased to lesser extents. To confirm the presence of GPI anchor on DAF and CD59b in sperm and testis from PGAP1 knock-out mice, we assessed the hydrophobicity of these proteins using Triton X-114 partitioning (Fig. 7*B*). Both proteins from PGAP1 knock-out and wild-type mouse testis and sperm were highly efficiently recovered in the detergent phase, indicating that DAF and CD59b were GPI-anchored in PGAP1 knock-out sperm.

DISCUSSION

We found at least three phenotypes in PGAP1 knock-out mice: a developmental defect (otocephaly), growth retardation, and male infertility. Otocephaly or agnathia of mouse was reported to be caused by the defects of several genes like *oto* (27) and *Otx2* (38–42). How these genes affect the craniofacial formation of mice is still unclear, but Wnt proteins are suggested to be affected by Otx2 (43). In the processes of mouse embryonic development, the embryonic axis is first generated in a proximal-distal direction by embryonic day 5.5 (E5.5). The orientation of the axis is then changed to the anterior-posterior direction (44). This axis conversion requires the function of Otx2, a homeobox transcription factor, which is a murine orthologue of the *Drosophila* orthodenticle (otd) gene (45). Axis conversion failed in *Otx2* knock-out embryos, resulting in otocephaly (38, 39). Through examining the expression pattern of various marker genes for anterior visceral endoderm cells like *Lefty* or *Cerl*, it was found that a Wnt antagonist, Dickkopf1 (Dkk1), was not expressed in *Otx2* knock-out mice (38, 46, 47). Dkk1 inhibits Wnt-induced Frizzled-LRP5/6 complex formation, degrades β-catenin indirectly, and prevents Wnt signaling (48–52). The Wnt family is a well conserved cysteine-rich glycoprotein family among vertebrates, and it participates in various developmental events during embryogenesis (53, 54). Thus, it is hypothesized that the phenotype of the *Otx2* mutant is caused by the malfunction of anterior-posterior axis polarization by up-regulation of Wnt/β-catenin signaling due to Dkk1 deficiency. It is known that Wnt/β-catenin signaling is modulated by division abnormally delayed (Dally)-like proteins (Dlp) in *Drosophila* (55–61). Dally is one of the glypican members of *Drosophila* (56, 62, 63). Glypicans are a family of heparan sulfate proteoglycans attached to the cell surface via a GPI anchor.

The Journal of Biological Chemistry

Downloaded from www.jbc.org at Keio University Shinanomachi Media Center on March 6, 2008

Two glypican members, Dally and Dlp have been implicated in Wg signaling (55, 62, 64). In the imaginal disc of *Drosophila*, Dlp cooperates with Notum, an α/β-hydrolase enzyme with homology to plant pectin acetylesterases, to down-regulate Wg signaling (57, 65). For this down-regulation, Notum is believed to cleave the GPI portion of Dlp (65). If an acylated GPI anchor is resistant to this cleavage, a higher amount of Dlp might enhance Wg signaling. A similar relationship between Dlp and Notum has not been reported in mammals, but Wnt signaling could be controlled by the same mechanism. The participation of GPI-anchor cleavage in Wnt signaling remains to be elucidated.

Once PGAP1 pups have survived the critical period after birth, most of them showed no behavioral abnormality except growth retardation. The body sizes of three genotypes mice at 18.5 days post coitus weren't significantly different from each other, suggesting that the impaired growth curve of knock-out mice was caused by postnatal reasons. Further analysis is required to identify the underlying mechanism.

Our experiments revealed that PGAP1 knock-out sperm are defective in binding to the zona pellucida. One can argue that the impaired zona binding property may be derived from the impairment of sperm capacitation process done *in vitro*. However, the zona binding ability of sperm is evident even in the initial stage of incubation in TYH medium or "capacitating medium." Together with the result that the sperm from PGAP1 null mice underwent normal acrosome reaction estimated from the normal fusing ability, we presume that the decreased zona binding ability is a characteristic of sperm relating to the change of membrane constitution rather than the impaired sperm capacitation process.

There were higher amounts of several GPI-APs on sperm of PGAP1 knock-out mice as detected by Western blotting. We compared CD48 and DAF expression on the surfaces of mononuclear cells of peripheral blood between wild-type mice and PGAP1 knock-out mice, as well as PGAP1-deficient Chinese hamster ovary cells, but no significant difference was observed (data not shown) (10). Thus, those higher expression levels seem unique to sperm. Many GPI-APs, including CD52, DAF, and CD59, are secreted from the male genital tracts and transferred to the surface of sperm, probably in the form of prostasomes (66–68), and GPI-APs like CD52 and P34H were reported to be transferred from epididymis epithelial cells to the sperm surface in the form of epididymosomes (69). The increased levels of GPI-APs, especially CD52 and DAF, on PGAP1 knock-out sperm are therefore likely due to efficient transfer. A three-"footed" anchor structure of GPI-APs in PGAP1 knock-out mice may have a higher tendency to be transferred to the sperm membrane, or be resistant to lipase (including GPI-cleaving enzyme), resulting in the higher amount of expression detected by Western blotting. Does this cause the infertility? We hypothesize that some GPI-APs should be decreased in the amount for efficient fertilization. Sperm need to undergo several phases of maturation, including capacitation (70, 71). Before capacitation, sperm maturation inhibitory components called decapacitation factors should be removed from the surface of sperm (72, 73). One decapacitation factor has been studied by Fraser *et al.* (72, 74), and its receptor on the sperm surface was reported to be a GPI-AP (75). Such three-footed inhibitory factor receptors might be transferred more in PGAP1-deficient mice than in wild-type mice, hindering sperm-egg interactions. Another possibility is that those GPI-anchored inhibitory components might not be properly removed in the process of sperm maturation. It was reported that ACE is indispensable for fertilization (36, 76) and that the cleavage of GPI-APs by ACE is important for male fertility (77). Three-footed GPI anchors might be resistant to this cleavage. It is also possible that signal transduction through membrane rafts is disturbed. A lack of deacylation of the GPI anchor may abolish the following fatty acid remodeling in the Golgi, which is critical for raft association of GPI-APs (78). This alters the localization of the GPI anchor on the membrane and might change GPI anchor-mediated signal transduction. As a general issue, the resistance to GPI-cleaving enzyme and altered localization and signaling of GPI caused by lack of deacylation could result in phenotypes, including otocephaly.

We found three phenotypes of PGAP1 knock-out mice, but their molecular mechanisms are still under investigation. Further analysis will reveal molecules involved in those phenotypes and the physiological importance of deacylation of GPI.

Acknowledgments—We thank Fumiko Mori and Keiko Kinoshita for excellent technical assistance.

REFERENCES

1. Tiede, A., Bastisch, I., Schubert, J., Orlean, P., and Schmidt, R. E. (1999) *Biol. Chem.* **380,** 503–523
2. McConville, M. J., and Menon, A. K. (2000) *Mol. Membr. Biol.* **17,** 1–16
3. Ikezawa, H. (2002) *Biol. Pharm. Bull.* **25,** 409–417
4. Ferguson, M. A., and Williams, A. F. (1988) *Annu. Rev. Biochem.* **57,** 285–320
5. Ferguson, M. A. (1999) *J. Cell Sci.* **112,** 2799–2809
6. Kinoshita, T., and Inoue, N. (2000) *Curr. Opin. Chem. Biol.* **4,** 632–638
7. Nozaki, M., Ohishi, K., Yamada, N., Kinoshita, T., Nagy, A., and Takeda, J. (1999) *Lab. Invest.* **79,** 293–299
8. Murakami, Y., Siripanyapinyo, U., Hong, Y., Kang, J. Y., Ishihara, S., Nakakuma, H., Maeda, Y., and Kinoshita, T. (2003) *Mol. Biol. Cell* **14,** 4285–4295
9. Chen, R., Walter, E. I., Parker, G., Lapurga, J. P., Millan, J. L., Ikehara, Y., Udenfriend, S., and Medof, M. E. (1998) *Proc. Natl. Acad. Sci. U. S. A.* **95,** 9512–9517
10. Tanaka, S., Maeda, Y., Tashima, Y., and Kinoshita, T. (2004) *J. Biol. Chem.* **279,** 14256–14263
11. Brown, D. A., and Rose, J. K. (1992) *Cell* **68,** 533–544
12. Simons, K., and Ikonen, E. (1997) *Nature* **387,** 569–572
13. Simons, K., and Toomre, D. (2000) *Nat. Rev. Mol. Cell. Biol.* **1,** 31–39
14. Mayor, S., and Riezman, H. (2004) *Nat. Rev. Mol. Cell. Biol.* **5,** 110–120
15. Zurzolo, C., Lisanti, M. P., Caras, I. W., Nitsch, L., and Rodriguez-Boulan, E. (1993) *J. Cell Biol.* **121,** 1031–1039
16. Walter, E. I., Roberts, W. L., Rosenberry, T. L., Ratnoff, W. D., and Medof, M. E. (1990) *J. Immunol.* **144,** 1030–1036
17. Deeg, M. A., Humphrey, D. R., Yang, S. H., Ferguson, T. R., Reinhold, V. N., and Rosenberry, T. L. (1992) *J. Biol. Chem.* **267,** 18573–18580
18. Rudd, P. M., Morgan, B. P., Wormald, M. R., Harvey, D. J., van den Berg, C. W., Davis, S. J., Ferguson, M. A., and Dwek, R. A. (1997) *J. Biol. Chem.* **272,** 7229–7244
19. Ikawa, M., Nakanishi, T., Yamada, S., Wada, I., Kominami, K., Tanaka, H., Nozaki, M., Nishimune, Y., and Okabe, M. (2001) *Dev. Biol.* **240,** 254–261
20. Toyoda, Y., Yokoyama, M., and Hoshi, T. (1971) *Jpn. J. Anim. Reprod.* **16,** 147–151

Downloaded from www.jbc.org at Keio University Shinanomachi Media Center on March 6, 2008

21. Yamagata, K., Nakanishi, T., Ikawa, M., Yamaguchi, R., Moss, S. B., and Okabe, M. (2002) *Dev. Biol.* **250,** 348–357
22. Baba, D., Kashiwabara, S., Honda, A., Yamagata, K., Wu, Q., Ikawa, M., Okabe, M., and Baba, T. (2002) *J. Biol. Chem.* **277,** 30310–30314
23. Yamaguchi, R., Yamagata, K., Ikawa, M., Moss, S. B., and Okabe, M. (2006) *Biol. Reprod.* **75,** 760–766
24. Ohta, R., Imai, M., Fukuoka, Y., Miwa, T., Okada, N., and Okada, H. (1999) *Microbiol. Immunol.* **43,** 1045–1056
25. Inoue, N., Ikawa, M., Isotani, A., and Okabe, M. (2005) *Nature* **434,** 234–238
26. Harris, C. L., Hanna, S. M., Mizuno, M., Holt, D. S., Marchbank, K. J., and Morgan, B. P. (2003) *Immunology* **109,** 117–126
27. Juriloff, D. M., Sulik, K. K., Roderick, T. H., and Hogan, B. K. (1985) *J. Craniofac. Genet. Dev. Biol.* **5,** 121–145
28. Bixler, D., Ward, R., and Gale, D. D. (1985) *J. Craniofac. Genet. Dev. Biol. Suppl.* **1,** 241–249
29. Winter, R. M. (1996) *Nat. Genet.* **12,** 124–129
30. Wallis, D., and Muenke, M. (2000) *Hum. Mutat.* **16,** 99–108
31. Ikawa, M., Wada, I., Kominami, K., Watanabe, D., Toshimori, K., Nishimune, Y., and Okabe, M. (1997) *Nature* **387,** 607–611
32. Nishimura, H., Kim, E., Nakanishi, T., and Baba, T. (2004) *J. Biol. Chem.* **279,** 34957–34962
33. Cho, C., Bunch, D. O., Faure, J. E., Goulding, E. H., Eddy, E. M., Primakoff, P., and Myles, D. G. (1998) *Science* **281,** 1857–1859
34. Shamsadin, R., Adham, I. M., Nayernia, K., Heinlein, U. A., Oberwinkler, H., and Engel, W. (1999) *Biol. Reprod.* **61,** 1445–1451
35. Nishimura, H., Cho, C., Branciforte, D. R., Myles, D. G., and Primakoff, P. (2001) *Dev. Biol.* **233,** 204–213
36. Hagaman, J. R., Moyer, J. S., Bachman, E. S., Sibony, M., Magyar, P. L., Welch, J. E., Smithies, O., Krege, J. H., and O'Brien, D. A. (1998) *Proc. Natl. Acad. Sci. U. S. A.* **95,** 2552–2557
37. Kessler, S. P., Rowe, T. M., Gomos, J. B., Kessler, P. M., and Sen, G. C. (2000) *J. Biol. Chem.* **275,** 26259–26264
38. Perea-Gomez, A., Lawson, K. A., Rhinn, M., Zakin, L., Brulet, P., Mazan, S., and Ang, S. L. (2001) *Development* **128,** 753–765
39. Kimura, C., Yoshinaga, K., Tian, E., Suzuki, M., Aizawa, S., and Matsuo, I. (2000) *Dev. Biol.* **225,** 304–321
40. Matsuo, I., Kuratani, S., Kimura, C., Takeda, N., and Aizawa, S. (1995) *Genes Dev.* **9,** 2646–2658
41. Hide, T., Hatakeyama, J., Kimura-Yoshida, C., Tian, E., Takeda, N., Ushio, Y., Shiroishi, T., Aizawa, S., and Matsuo, I. (2002) *Development* **129,** 4347–4357
42. Suda, Y., Matsuo, I., Kuratani, S., and Aizawa, S. (1996) *Genes. Cells* **1,** 1031–1044
43. Kimura-Yoshida, C., Nakano, H., Okamura, D., Nakao, K., Yonemura, S., Belo, J. A., Aizawa, S., Matsui, Y., and Matsuo, I. (2005) *Dev. Cell* **9,** 639–650
44. Beddington, R. S., and Robertson, E. J. (1999) *Cell* **96,** 195–209
45. Simeone, A., Acampora, D., Gulisano, M., Stornaiuolo, A., and Boncinelli, E. (1992) *Nature* **358,** 687–690
46. Kimura, C., Shen, M. M., Takeda, N., Aizawa, S., and Matsuo, I. (2001) *Dev. Biol.* **235,** 12–32
47. Zakin, L., Reversade, B., Virlon, B., Rusniok, C., Glaser, P., Elalouf, J. M., and Brulet, P. (2000) *Proc. Natl. Acad. Sci. U. S. A.* **97,** 14388–14393
48. Semenov, M. V., Tamai, K., Brott, B. K., Kuhl, M., Sokol, S., and He, X. (2001) *Curr. Biol.* **11,** 951–961
49. Bafico, A., Liu, G., Yaniv, A., Gazit, A., and Aaronson, S. A. (2001) *Nat. Cell Biol.* **3,** 683–686
50. Mao, B., Wu, W., Li, Y., Hoppe, D., Stannek, P., Glinka, A., and Niehrs, C. (2001) *Nature* **411,** 321–325
51. Mao, B., Wu, W., Davidson, G., Marhold, J., Li, M., Mechler, B. M., Delius, H., Hoppe, D., Stannek, P., Walter, C., Glinka, A., and Niehrs, C. (2002) *Nature* **417,** 664–667
52. Glinka, A., Wu, W., Delius, H., Monaghan, A. P., Blumenstock, C., and Niehrs, C. (1998) *Nature* **391,** 357–362
53. Logan, C. Y., and Nusse, R. (2004) *Annu. Rev. Cell Dev. Biol.* **20,** 781–810
54. Gordon, M. D., and Nusse, R. (2006) *J. Biol. Chem.* **281,** 22429–22433
55. Tsuda, M., Kamimura, K., Nakato, H., Archer, M., Staatz, W., Fox, B., Humphrey, M., Olson, S., Futch, T., Kaluza, V., Siegfried, E., Stam, L., and Selleck, S. B. (1999) *Nature* **400,** 276–280
56. Khare, N., and Baumgartner, S. (2000) *Mech. Dev.* **99,** 199–202
57. Kirkpatrick, C. A., Dimitroff, B. D., Rawson, J. M., and Selleck, S. B. (2004) *Dev. Cell.* **7,** 513–523
58. Kreuger, J., Perez, L., Giraldez, A. J., and Cohen, S. M. (2004) *Dev. Cell* **7,** 503–512
59. Franch-Marro, X., Marchand, O., Piddini, E., Ricardo, S., Alexandre, C., and Vincent, J. P. (2005) *Development* **132,** 659–666
60. Han, C., Yan, D., Belenkaya, T. Y., and Lin, X. (2005) *Development* **132,** 667–679
61. Hufnagel, L., Kreuger, J., Cohen, S. M., and Shraiman, B. I. (2006) *Dev. Biol.* **300,** 512–522
62. Baeg, G. H., Lin, X., Khare, N., Baumgartner, S., and Perrimon, N. (2001) *Development* **128,** 87–94
63. Nakato, H., Futch, T. A., and Selleck, S. B. (1995) *Development* **121,** 3687–3702
64. Lin, X., and Perrimon, N. (1999) *Nature* **400,** 281–284
65. Giraldez, A. J., Copley, R. R., and Cohen, S. M. (2002) *Dev. Cell* **2,** 667–676
66. Kirchhoff, C., and Hale, G. (1996) *Mol. Hum. Reprod.* **2,** 177–184
67. Rooney, I. A., Heuser, J. E., and Atkinson, J. P. (1996) *J. Clin. Invest.* **97,** 1675–1686
68. Kravets, F. G., Lee, J., Singh, B., Trocchia, A., Pentyala, S. N., and Khan, S. A. (2000) *Prostate* **43,** 169–174
69. Saez, F., Frenette, G., and Sullivan, R. (2003) *J. Androl.* **24,** 149–154
70. Austin, C. R. (1952) *Nature* **170,** 326
71. de Lamirande, E., Leclerc, P., and Gagnon, C. (1997) *Mol. Hum. Reprod.* **3,** 175–194
72. Fraser, L. R. (1984) *J. Reprod. Fertil.* **72,** 373–384
73. Bedford, J. M., and Chang, M. C. (1962) *Am. J. Physiol.* **202,** 179–181
74. Fraser, L. R. (1998) *Mol. Reprod. Dev.* **51,** 193–202
75. Gibbons, R., Adeoya-Osiguwa, S. A., and Fraser, L. R. (2005) *Reproduction* **130,** 497–508
76. Krege, J. H., John, S. W., Langenbach, L. L., Hodgin, J. B., Hagaman, J. R., Bachman, E. S., Jennette, J. C., O'Brien, D. A., and Smithies, O. (1995) *Nature* **375,** 146–148
77. Kondoh, G., Tojo, H., Nakatani, Y., Komazawa, N., Murata, C., Yamagata, K., Maeda, Y., Kinoshita, T., Okabe, M., Taguchi, R., and Takeda, J. (2005) *Nat. Med.* **11,** 160–166
78. Maeda, Y., Tashima, Y., Houjou, T., Fujita, M., Yoko-o, T., Jigami, Y., Taguchi, R., and Kinoshita, T. (2007) *Mol. Biol. Cell* **18,** 1497–1506

Downloaded from www.jbc.org at Keio University Shinanomachi Media Center on March 6, 2008

STEM CELLS
EMBRYONIC STEM CELLS

Efficient Derivation of Embryonic Stem Cells by Inhibition of Glycogen Synthase Kinase-3

HIROKI UMEHARA,[a] TOHRU KIMURA,[b] SATOSHI OHTSUKA,[c] TOSHINOBU NAKAMURA,[a] KENJI KITAJIMA,[b] MASAHITO IKAWA,[d] MASARU OKABE,[d] HITOSHI NIWA,[c,e] TORU NAKANO[a,b]

[a]Graduate School of Frontier Biosciences, [b]Department of Pathology, Graduate School of Medicine, Osaka University, Osaka, Japan; [c]Laboratory for Pluripotent Cell Studies, RIKEN Center for Developmental Biology, Kobe, Japan; [d]Genome Information Research Center, Institute for Microbial Diseases, Osaka University, Osaka, Japan; and [e]Department of Developmental and Regenerative Medicine, Graduate School of Medicine, Kobe University, Kobe, Japan

Key Words. Embryonic stem cells • Glycogen synthase kinase-3 • Akt • Pluripotency • Stem cells

ABSTRACT

Embryonic stem (ES) cells are derived from the inner cell mass (ICM) of blastocysts. The use of ES cells as a source of differentiated cells holds great promise for cell transplantation therapy. The efficiency of ES cell derivation is affected by genetic variation in mice; that is, some mouse strains, such as C57BL/6, are amenable to ES cell derivation, whereas others, such as BALB/c, are refractory. Developing an efficient method to establish ES cells from strains of various genetic backgrounds should be valuable for derivation of ES cells in various mammalian species, including human. Although it is well-established that various signaling pathways, including phosphoinositide 3-kinase (PI3K)/Akt and Wnt/β-catenin, regulate the maintenance of ES cell pluripotency, little is known about the signaling pathways involved in the derivation of ES cells from ICMs. In this study, we demonstrated that inhibition of glycogen synthase kinase-3 (GSK-3), one of the crucial molecules in the regulation of the Wnt/β-catenin, Hedgehog, and Notch signaling pathways, dramatically augmented ES cell derivation from both C57BL/6 and BALB/c mouse strains. In contrast, Akt signaling activation enhanced the growth of ICM but did not increase the efficiency of ES cell derivation. Our study establishes an efficient means for ES cell derivation by pharmacological inhibition of GSK-3. STEM CELLS *2007;25: 2705–2711*

Disclosure of potential conflicts of interest is found at the end of this article.

INTRODUCTION

Embryonic stem (ES) cell lines have been established from several mammalian species, including mouse, monkey, and human [1, 2]. Although ES cell lines have been derived in many laboratories, the success rate for derivation is variable, probably reflecting differences in embryo quality, derivation methods, and genetic background [3]. For instance, mouse strains such as C57BL/6 are amenable to establishing ES cell lines, whereas strains such as BALB/c, Institute for Cancer Research, and nonobese diabetic are refractory [4, 5].

The mechanisms that sustain ES cell pluripotency in culture have been investigated extensively. Pluripotency can be maintained by leukemia inhibitory factor (LIF) in mouse ES cells. The downstream activation of signal transducer and activator of transcription-3 (STAT3) is essential for LIF action [6–8]. Despite its crucial roles in mice, STAT3 activation is not involved in the maintenance of primate ES cell pluripotency [9, 10]. In contrast, the pluripotency of both mouse and human ES cells can be maintained by inhibition of glycogen synthase kinase-3 (GSK-3), which was revealed by its specific inhibitor [11]. Activation of Wnt/β-catenin signaling is caused by the GSK-3 inhibitor and could play important roles in the maintenance of ES cell pluripotency. However, the involvement of Wnt/β-catenin signaling in the maintenance of ES cell pluripotency is controversial, because addition of recombinant Wnt3a stimulates human ES cell differentiation and is not sufficient for maintaining mouse ES cell pluripotency [12, 13]. Other GSK-3 targets, such as the Hedgehog and Notch signaling pathways, may cooperatively regulate pluripotency. Meanwhile, the activation of phosphoinositide 3-kinase (PI3K) and the downstream serine-threonine kinase Akt plays a critical role in the maintenance of ES cell pluripotency. Pharmacological inhibition of PI3K induces differentiation of mouse ES cells, and introduction of the active form of Akt maintains pluripotency in mouse and primate ES cells [14, 15].

In contrast to the extensive study on the molecular basis for sustaining ES cell pluripotency [16, 17], the mechanisms underlying the derivation of ES cell lines from epiblasts remain poorly understood. In this study, we investigated the effects of GSK-3 and Akt signaling on the derivation of ES cells from the inner cell mass (ICM). Inhibition of GSK-3 signaling but not activation of Akt signaling augmented the efficiency of ES cell derivation in mice. Our pharmacological approach using a GSK-3 inhibitor potentially provides a general strategy to improve ES cell derivation from diverse mammalian species.

MATERIALS AND METHODS

Mice and Embryos

Two-cell embryos were obtained from C57BL/6 and BALB/c inbred strains. Embryos were also isolated from a cross between Akt-Mer transgenic male mice of a C57BL/6-DBA2 mixed back-

Correspondence: Toru Nakano, M.D., Ph.D., Department of Pathology, Graduate School of Medicine, Graduate School of Frontier Biosciences, Osaka University, 2-2 Yamada-oka, Suita, Osaka, Japan 565-0871. Telephone: 81-6-6879-3720; Fax: 81-6-6879-3729; e-mail: tnakano@patho.med.osaka-u.ac.jp Received January 31, 2007; accepted for publication July 9, 2007; first published online in STEM CELLS *Express* July 19, 2007. ©AlphaMed Press 1066-5099/2007/$30.00/0 doi: 10.1634/stemcells.2007-0086

Downloaded from www.StemCells.com at Keio University Shinanomachi Media Center on March 6, 2008

Table 1. Oligonucleotides primers used for reverse transcription-PCR analysis

Gene	Sense	Antisense	PCR cycles
Mixl1	5'-ACTTTCCAGCTCTTTCAAGAGCC-3'	5'-ATTGTGTACTCCCCAACTTTCCC-3'	26
Brachyury	5'-AACTTTCCTCCATGTGCTGAGAC-3'	5'-TGACTTCCCAACACAAAAAGCT-3'	26
Collagen IV	5'-CAAGCATAGTGGTCCGAGTC-3'	5'-AGGCAGGTCAAGTTCTAGCG-3'	21
AFP	5'-TGCAGAAACACATCGAGGAGAG-3'	5'-GCTTCACCAGGTTAAGAGAAGCT-3'	30
Nestin	5'-AACTGGCACACCTCAAGATGT-3'	5'-TCAAGGGTATTAGGCAAGGGG-3'	24
GAPDH	5'-GGGTGGAGCCAAACGGGTCATC-3'	5'-GCCAGTGAGCTTCCCGTTCAGC-3'	18

Abbreviation: PCR, polymerase chain reaction.

ground and C57BL/6 female mice [18]. Female mice were superovulated by injection with pregnant mare serum gonadotropin (ASKA Pharmaceutical, Tokyo, http://www.aska-pharma.co.jp) followed by injection with human chorionic gonadotropin (ASKA Pharmaceutical) 48 hours later. Mice were kept on a 12-hour-light/12-hour-dark regimen. Twelve hours from the middle of the dark period was termed embryonic day 0.5 (E0.5). E13.5 fetuses from the ICR strain were used to obtain mouse embryonic fibroblasts (MEFs) for use as feeder cells. All animal studies were approved by the Animal Care and Use Committee of Osaka University.

Isolation of ICM

Two-cell-stage embryos (E1.5) were flushed from the oviducts into phosphate-buffered saline (PBS) with 10% fetal calf serum (FCS) and cultured for 3 days in Hepes-buffered potassium simplex-optimized medium (KSOM; Specialty Media, Phillipsburg, NJ, http://www.specialtymedia.com/) or KSOM supplemented with 4-hyroxytamoxifen (4OHT; Sigma-Aldrich, St. Louis, http://www.sigmaaldrich.com). Immunosurgery was performed on blastocysts as described previously [19]. Briefly, the zona pellucida was removed with acid-Tyrode's solution (Sigma-Aldrich), and the blastocysts were treated with rabbit anti-mouse red blood cell antibody (Inter-cell Technologies, Jupiter, FL) for 30 minutes in a CO_2 incubator at 37°C. After three washes with KSOM, embryos were treated with guinea pig complement (Merck, Darmstadt, Germany, http://www.merck.com) diluted in KSOM. Embryos were observed periodically under a dissecting microscope to check for lysis of trophectodermal cells. We usually observed membrane blebbing within 30 minutes. The ICM was then isolated and used for derivation of ES cell lines.

Derivation and Culture of ES Cell Lines

The ES culture medium was Glasgow minimal essential medium supplemented with 20% knockout serum replacement (Gibco-BRL, Gaithersburg, MD, http://www.gibcobrl.com), 0.3% FCS (Sigma-Aldrich), 2-mercaptoethanol (Sigma-Aldrich), antibiotics (Sigma-Aldrich), nonessential amino acids (Gibco-BRL), pyruvate (Gibco-BRL), and LIF. 6-Bromoindirubin-3'-oxime (BIO; Merck), methyl-BIO (Me-BIO; Merck), or 4OHT was supplemented in the ES medium. The isolated ICMs were seeded onto MEFs and cultured for 6 days. The expanded ICMs were dissociated individually into fresh wells and cultured for 5 days. When ES colonies were visible, the cells were trypsinized and replated in 35-mm dishes with fresh feeders.

Immunostaining

Cells were fixed with 4% paraformaldehyde (PFA) in PBS for 10 minutes at room temperature and permeabilized with 0.2% Triton X-100 in PBS for 10 minutes. The blocking solution consisted of 5% normal goat serum with 0.2% Tween 20 in PBS and was used for 30 minutes at room temperature. Anti-Oct-3/4 (1:200; Santa Cruz Biotechnology Inc., Santa Cruz, CA, http://www.scbt.com), stage-specific embryonic antigen-1 (1:50; Kyowa Hakko, Tokyo, http://www.kyowa.co.jp/eng/), α-smooth muscle actin (DAKO, Glostrup, Denmark, http://www.dako.com), α-fetoprotein (DAKO), type II collagen (1:100; Chemicon, Temecula, CA, http://www.chemicon.com), and pancytokeratin (1:200; Sigma-Aldrich) were used as primary antibodies. Alexa Fluor 568-conjugated and Alexa Fluor 488-conjugated antibodies (1:200; Invitrogen, Carlsbad, CA, http://www.invitrogen.com) were used as secondary antibodies to detect primary antibody complexes.

In Vitro Differentiation Assays

In vitro differentiation induction of ES cells into hematopoietic cells was performed as previously described [20]. For EB formation, ES cells were trypsinized, resuspended in ES culture medium without LIF, and replated on bacteriological dishes at a density of 1.6×10^5 cells per cm^2. Cells were refed every second day and cultured for 7 days in suspension. The resultant cystic EBs were then adhered to gelatin-coated dishes and cultured for an additional 7 days. Total RNA was prepared from the EBs at days 0, 3, 5, 7, 10, and 14 after differentiation induction.

Reverse Transcription-Polymerase Chain Reaction

Total RNA was isolated by an RNeasy mini kit (Qiagen, Valencia, CA, http://www1.qiagen.com), and 1 μg of total RNA was used for cDNA synthesis. The reverse transcription was performed using the ThermoScript reverse transcription-polymerase chain reaction (RT-PCR) system (Gibco-BRL) as described [21]. PCRs were optimized to allow semiquantitative comparisons within the log phase of amplification. The primer sequences and amplification cycles are listed in Table 1. The PCR products were analyzed by agarose gel electrophoresis and visualized using ethidium bromide staining. The intensity of bands was quantified by NIH ImageJ (http://rsb.info.nih.gov/nih-image) and normalized against *GAPDH*.

Teratoma Formation

ES cells (5×10^6) were injected subcutaneously into nude mice. After 3 weeks, the teratoma were excised, fixed in 4% PFA, and subjected to histological examination with H&E, periodic acid-Schiff (PAS), Alcian Blue, and immunostaining.

Production of Chimeric Mice

ES cells derived from C57BL/6 (coat color, black) and BALB/c (coat color, white) strains were injected into the blastocele of recipient blastocyst-stage embryos from BALB/c and C57BL/6 strains, respectively. The incorporation of cells into the chimeric mice was monitored by coat color. Germline transmission was then tested by crossing the chimeras with ICR strains (coat-color genotype, AA/bb/cc). Germline transmission of the C57BL/6 cells (aa/BB/CC) produces the offspring with agouti coat color (Aa/Bb/Cc), whereas the transmission of the BALB/c cells (AA/bb/cc) produces offspring with white coat color (AA/bb/cc).

Results

Augmentation of ES Cell Derivation by Pharmacological Inhibition of GSK-3

We investigated the impact of GSK-3 inhibition on ES cell derivation using the specific inhibitor BIO or its inactivated derivative, Me-BIO [22]. The experimental scheme for ES cell derivation used in this study is illustrated in Figure 1A. Two-cell-stage embryos were recovered at E1.5 from superovulated C57BL/6 female mice and cultured for 3 days to the blastocyst

Downloaded from www.StemCells.com at Keio University Shinanomachi Media Center on March 6, 2008

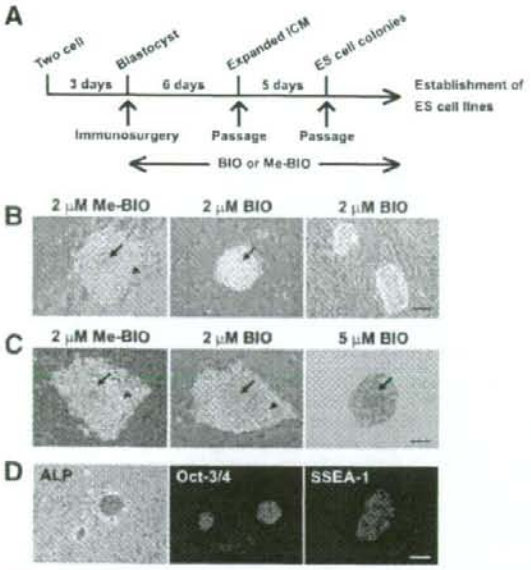

Figure 1. ES cell derivation by treatment with glycogen synthase kinase-3 inhibitor. **(A):** Experimental scheme of ES cell derivation. Two-cell-stage embryos were developed to the blastocyst stage by culturing for 3 days in potassium simplex-optimized medium in vitro. The ICMs isolated from blastocysts by immunosurgery were seeded onto mouse embryonic fibroblasts (MEFs) and allowed to expand for 6 days. The expanded ICMs were dissociated individually onto fresh MEFs and cultured for 5 days. The colonies with ES-like morphology were then selected for further propagation and characterization. BIO treatment was started at the beginning of the ICM culture and was continued until ES establishment. **(B):** Expanded ICMs (left and middle) and ES cell colonies (right) derived from C57BL/6 mice cultured in the presence of 2 μM Me-BIO and 2 μM BIO. BIO treatment did not affect proliferation of epiblasts but suppressed endodermal growth in the ICM cultures. Arrow and arrowhead represent the epiblasts and endodermal cells, respectively. **(C):** Expanded ICM colonies derived from BALB/c mice cultured in the presence of 2 μM Me-BIO, 2 μM BIO, and 5 μM BIO. Augmentation of ES cell derivation was correlated with the suppression of endodermal cells. Arrow and arrowhead represent the epiblasts and endodermal cells, respectively. **(D):** ES cell lines established from BALB/c mice in the presence of 5 μM BIO. These cells expressed undifferentiated-ES-cell markers, such as ALP, Oct-3/4, and stage-specific embryonic antigen-1. Scale bars = 100 μm **(B–D)**. Abbreviations: ALP, alkaline phosphatase; BIO, 6-bromoindirubin-3′-oxime; ES, embryonic stem; ICM, inner cell mass; Me-BIO, methyl-6-bromoindirubin-3′-oxime.

stage without BIO. The ICMs were isolated by immunosurgery and plated onto feeder layers of MEFs. Culture of the ICMs was conducted in the presence of LIF and BIO until the establishment of ES cell lines. At day 6 after seeding on MEFs, approximately 30% of the ICMs attached and proliferated to form large expanded ICM colonies, which consisted of proliferating epiblasts inside and growing primitive endoderm outside (Fig. 1B; Table 2). In the culture treated with 2 μM BIO, approximately 80% of the ICMs expanded to form colonies, and outgrowth of the primitive endoderm was suppressed (Fig. 1B). The expanded ICMs were picked up, trypsinized, and passed onto MEFs to establish ES cell lines. When treated with BIO, nearly all of the expanded ICM colonies (34 of 35) gave rise to ES cell lines (Fig. 1B; Table 2). In total, the efficiency of ES cell derivation increased by approximately fourfold with 2 μM BIO treatment in C57BL/6 mice.

The BALB/c mouse strain is reportedly refractory for ES cell derivation [4, 5]. Indeed, ES cell colonies emerged from the ICM culture of BALB/c embryos, but only a small number of ES cell lines could be stably propagated (Table 2). Similarly, treatment with 2 μM BIO did not facilitate ES cell derivation in BALB/c embryos. The endodermal cells in the BIO-treated ICM colonies proliferated extensively, as did control ICMs (Fig. 1C). However, when the concentration of BIO was increased to 5 μM, endodermal outgrowth was suppressed (Fig. 1C) and ES cell lines were established from more than 30% of the embryos (Table 2). Once established, these cells proliferated indefinitely, retaining the characteristics of undifferentiated ES cells in the absence of BIO (Fig. 1D). These results clearly demonstrate that ES cell derivation is augmented by inhibition of GSK-3, regardless of genetic background.

Table 2. Efficiency of ES cell derivation by treatment with glycogen synthase kinase-3 inhibitor

Mouse strain	Treatment[a]	ICM	Expanded ICM	ES cell lines	Efficiency (%)[b]
C57BL/6	2 μM Me-BIO	45	13	9	20
	2 μM BIO	45	35	34	76[c]
BALB/c	2 μM Me-BIO	36	15	2	6
	5 μM Me-BIO	35	12	3	9
	2 μM BIO	25	19	1	4
	5 μM BIO	67	25	21	31[c]

[a]Treatment was started in the blastocyst stage.
[b]Efficiency of ES cell establishment was calculated by dividing the number of established ES cell lines by the total number of ICMs.
[c]Efficiency was statistically higher than in the corresponding Me-BIO group. $p < 0.0005$ by the χ^2 test.
Abbreviations: BIO, 6-bromoindirubin-3′-oxime; ES, embryonic stem; ICM, inner cell mass; Me-BIO, methyl-6-bromoindirubin-3′-oxime.

We next examined the effects of Akt signaling activation on the efficiency of ES cell derivation (details given in supplemental online data). For this purpose, we used transgenic mice expressing the Akt-Mer chimeric protein (C57BL/6-DBA2 mixed background) [18], which allowed us to control Akt signaling activation in a conditional manner by the addition or removal of 4OHT. When Akt signaling was activated from the two-cell stage, both the cell size and the cell number increased in the isolated ICMs (supplemental online Fig. 1). However, the efficiency of ES cell derivation was not altered by the activation of Akt even in the case in which activation was induced during the entire derivation process (supplemental online Table 1).

Multipotent Differentiation Capacities of the Established ES Cell Lines

Differentiation capacities of the ES cell lines established with BIO were first evaluated by in vitro differentiation assays. The EBs were generated from the ES cells established from both C57BL/6 and BALB/c strains. As shown in Figure 2A, the vast majority of EBs did not contain the Oct3/4-positive cells at day 6 after differentiation induction, indicating that differentiation took place uniformly in the EBs. There were no significant differences between the ES cells that were established in the presence of BIO and those established in the presence of Me-BIO. α-Fetoprotein (AFP)-positive cells and α-smooth muscle actin-positive cells were detected in some fraction of EBs, as shown in Figure 2B.

To determine the differentiation capacities quantitatively, we examined the marker gene expression in a long-term EB differentiation system. The ES cells were applied to suspension cultures to produce EBs for 7 days and then adhered to gelatin-coated plates and differentiated for an additional 7 days. Ex-

Downloaded from www.StemCells.com at Keio University Shinanomachi Media Center on March 6, 2008

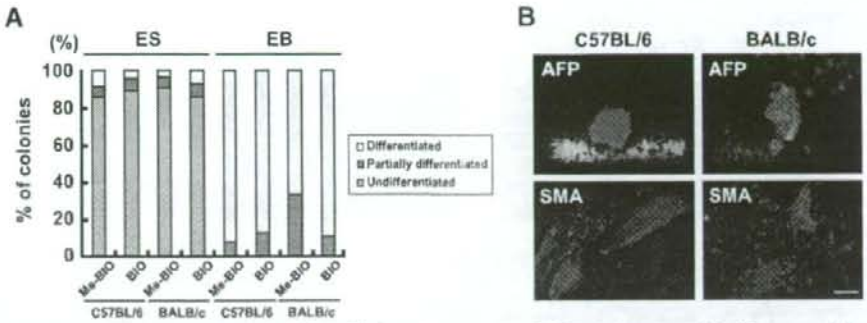

Figure 2. Differentiation of ES cells established with BIO in EB formation assay. **(A):** Differentiation status of the EBs generated from the ES cells established with Me-BIO or BIO. The EBs at day 6 after differentiation induction were stained with anti-Oct3/4 antibody. The EBs that had a small number of Oct3/4-positive cells were counted as partially differentiated EBs. Oct-3/4-positive cells were not detected in large portions of the EBs. The ES cells cultured with leukemia inhibitory factor were stained as a positive control. **(B):** Double immunostaining of the day 6 EBs with the antibodies against differentiation markers (AFP and α-SMA; red) and anti-Oct3/4 antibody (green). The EBs generated from C57BL/6 (left column) and BALB/c (right column) mouse strains were positive for AFP (top) and SMA (bottom). The signals for Oct-3/4 were not detectable. Scale bar = 100 μm. Abbreviations: AFP, α-fetoprotein; BIO, 6-bromoindirubin-3'-oxime; ES, embryonic stem; Me-BIO, methyl-6-bromoindirubin-3'-oxime; SMA, α-smooth muscle actin.

pression of the marker genes for three germ layers was analyzed by semiquantitative RT-PCR. We examined *Mixl1* and *Brachyury* as mesodermal markers, *Collagen IV* and *AFP* as endodermal markers, and *Nestin* as an ectodermal marker. As shown in Figure 3, the time courses and the maximal levels of the expression were slightly varied among the cell lines; expression of all the differentiation markers was efficiently induced in the ES cell lines established with BIO. Furthermore, in an in vitro hematopoietic differentiation system, the ES cells also differentiated into mesodermal colonies and then to various hematopoietic cells (Fig. 4A).

We next analyzed the multilineage differentiation capacities of the ES cell lines in vivo. When transplanted into nude mice, the ES cells established from both the C57BL/6 and the BALB/c strains produced various differentiated tissues, such as cartilage, mucosal gland, and epithelium (Fig. 4B–4D). The cartilage cells expressed chondrocyte marker type II collagen, and proteoglycan synthesis was shown by staining with Alcian Blue (Fig. 4B). The cells of mucosal glands expressed the epithelial marker cytokeratin (Fig. 4C). The cavities of the glands contained the materials stained with PAS and Alcian Blue, showing that the gland cells secreted acid mucin. The squamous epithelial cells were positive for cytokeratin and contained terminally differentiated stratum corneum (Fig. 4D). Thus, the ES cells established with BIO had the capacity to produce various tissue structures. Next, we examined the capacity to contribute to chimeric mice. Five C57BL/6 ES cell lines were injected into E3.5 BALB/c blastocysts. Two cell lines generated chimeric mice (Fig. 4E), and one line was transmitted through germline (Fig. 4F). The chimeric mice were also produced from two BALB/c ES cell lines out of three lines examined (Fig. 4E), but no germline transmission was observed. Taken together with the above in vitro and in vivo differentiation assays, our data indicate that the ES cells established by GSK-3 inhibition possessed pluripotent differentiation ability.

DISCUSSION

In this study, we analyzed the effects of GSK-3 inhibition and Akt activation on ES cell derivation from ICM cultures. First, we demonstrated that inhibition of GSK-3 with BIO augmented the efficiency of ES cell derivation, regardless of the mouse strain used. BIO treatment dramatically enhanced the efficiency of ES cell derivation from expanded ICMs in both C57BL/6 and BALB/c strains (Table 1). In addition, the emergence of expanded ICM colonies was also promoted by the BIO treatment in C57BL/6 mice. In contrast to GSK-3 inhibition, activation of Akt signaling did not show a supportive effect on ES cell derivation. However, the activation of Akt signaling increased the size and the number of ICM cells. Since the Akt-Mer transgenic mice had the C57BL/6-DBA/2 mixed background, the possibility could not be excluded that the difference in the efficiency of ES cell derivation between GSK-3 inhibition and Akt activation reflects the differences in the genetic background of the mice used.

Multipotent differentiation capacities of the ES cell lines established with BIO were shown by in vitro differentiation assays, teratoma formation in nude mice, and chimeric mouse production. Although the C57BL/6 ES cell line was successfully transmitted through germline, none of the BALB/c ES cell lines showed germline transmission. To our knowledge, only one report has demonstrated the germline transmission of BALB/c-derived ES cells [23]. The chromosomal instability is likely the major reason why BALB/c-derived ES cells failed to transmit through germline. Indeed, the BALB/c ES cell lines showed a higher percentage of aneuploidy than the C57BL/6 ES cells (data not shown). Thus, additional studies should be necessary to develop not only the methods to derive ES cells but also the procedures to maintain the normal karyotype of ES cells stably.

ICM cells differentiate to epiblasts and primitive endoderm. Epiblasts produce the entire fetus after implantation, whereas primitive endodermal cells contribute to the yolk sac. In the ICM cultures for ES cell derivation, a population of epiblasts within the ICM colonies gives rise to ES cell lines while maintaining the pluripotency. Considering the process of ES cell line establishment, BIO treatment presumably supports the pluripotency of epiblasts during the initial phase of culture.

How does GSK-3 inhibition improve the ES cell derivation? GSK-3 activates various signaling pathways, such as Wnt/β-catenin, Hedgehog, Notch, and protein kinase A (PKA) signals [24, 25]. It has been demonstrated that Wnt/β-catenin signaling is activated in BIO-treated ES cells [11]. However, Wnt/β-catenin signaling alone cannot account for the BIO-mediated maintenance of pluripotency because neither the addition of Wnt3a nor the introduction of stabilized β-catenin was sufficient to maintain the ES cell pluripotency [12, 13]. Hedgehog and Notch signaling pathways are also implicated in self-re-

Downloaded from www.StemCells.com at Keio University Shinanomachi Media Center on March 6, 2008

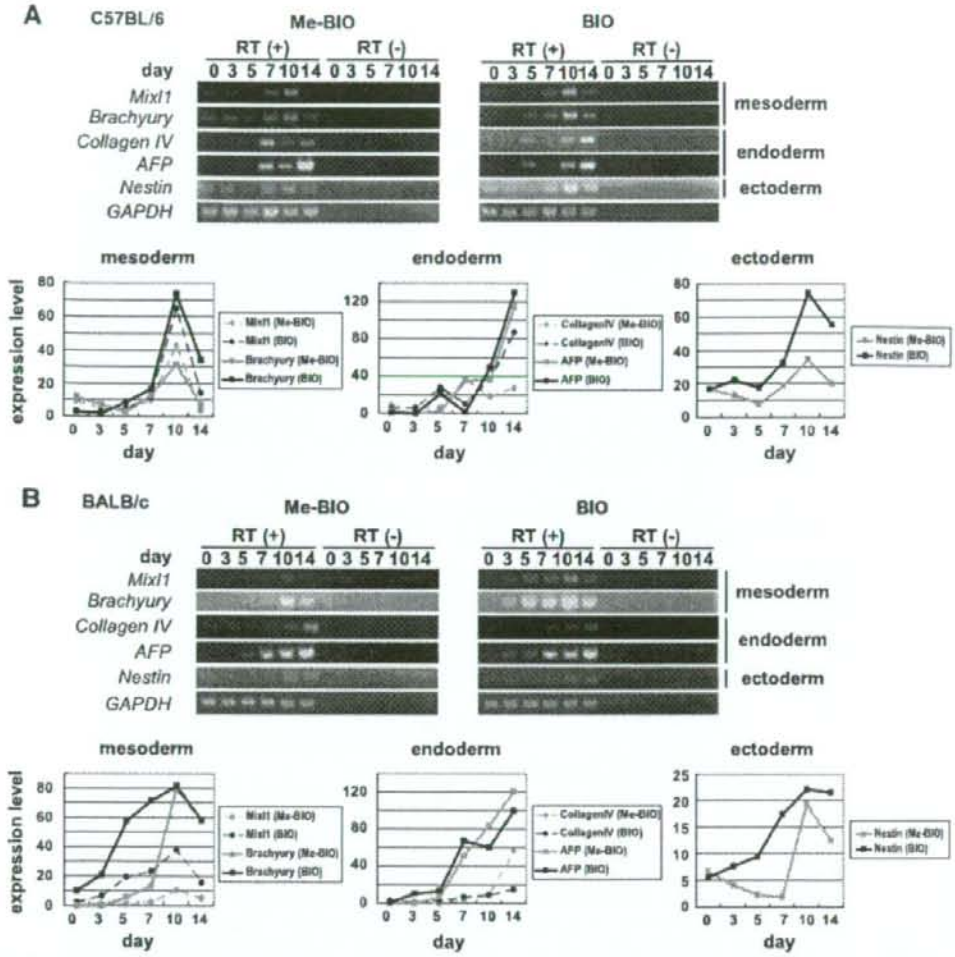

Figure 3. Expression of differentiation marker genes in the EB formation assay. Semiquantitative RT-polymerase chain reaction (RT-PCR) analysis of EBs generated from the embryonic stem (ES) cell lines established from C57BL/6 (**A**) and BALB/c (**B**) strains. Expression of the marker genes of three germ layers was analyzed by RT-PCR. The PCR products were run on agarose gel and visualized by staining with ethidium bromide. The intensity of each band was quantified and normalized against *GAPDH* expression. *Mixl1* and *Brachyury*, mesoderm markers; *Collagen IV* and *AFP*, endoderm markers; *Nestin*, ectoderm marker. Abbreviations: AFP, α-fetoprotein; BIO, 6-bromoindirubin-3′-oxime; Me-BIO, methyl-6-bromoindirubin-3′-oxime; RT, reverse transcription.

newal of tissue stem cells and cancer stem cells [26–30], suggesting that BIO-induced activation of these signals would play important roles in the efficient ES cell derivation.

Besides the signaling pathways, a number of proteins are regulated by GSK-3 through phosphorylation. c-Myc is an attractive candidate that may participate in the promotion of ES cell derivation. Enforced expression of c-Myc supports the mouse ES cell self-renewal in the absence of LIF [31] and reprograms fibroblasts to pluripotent stem cells in cooperation with Oct-3/4, Sox-2, and Klf4 [32]. Because GSK-3 induces c-Myc degradation through its phosphorylation, stabilization of c-Myc induced by GSK-3 inhibition would promote the ES cell derivation. When these data are taken together, it is conceivable that activation of several signaling pathways and stabilization of c-Myc cooperatively support the pluripotency of the epiblasts during the ES cell derivation.

GSK-3 activity is inhibited by Akt via direct phosphorylation. However, Akt activation does not seem to inactivate the entire pool of GSK-3. Introduction of activated Akt into ES cells induces hyperphosphorylation of GSK-3 but does not activate Wnt/β-catenin signaling [15], indicating that Akt activation cannot inactivate a fraction of GSK-3 within the β-catenin destruction complex in ES cells. In addition, GSK-3 is integrated into the protein complexes involved in the Hedgehog and PKA signaling pathways [24, 25]. The insulation of some fraction of GSK-3 from the Akt signal may explain why treatment with GSK-3 inhibitor but not Akt activation augments ES cell derivation.

BIO-augmented ES cell establishment was preceded by the suppression of endodermal outgrowth (Fig. 1B, 1C). The critical role of GSK-3 in primitive endodermal development was also demonstrated by the impaired primitive endodermal growth in

Downloaded from www.StemCells.com at Keio University Shinanomachi Media Center on March 6, 2008

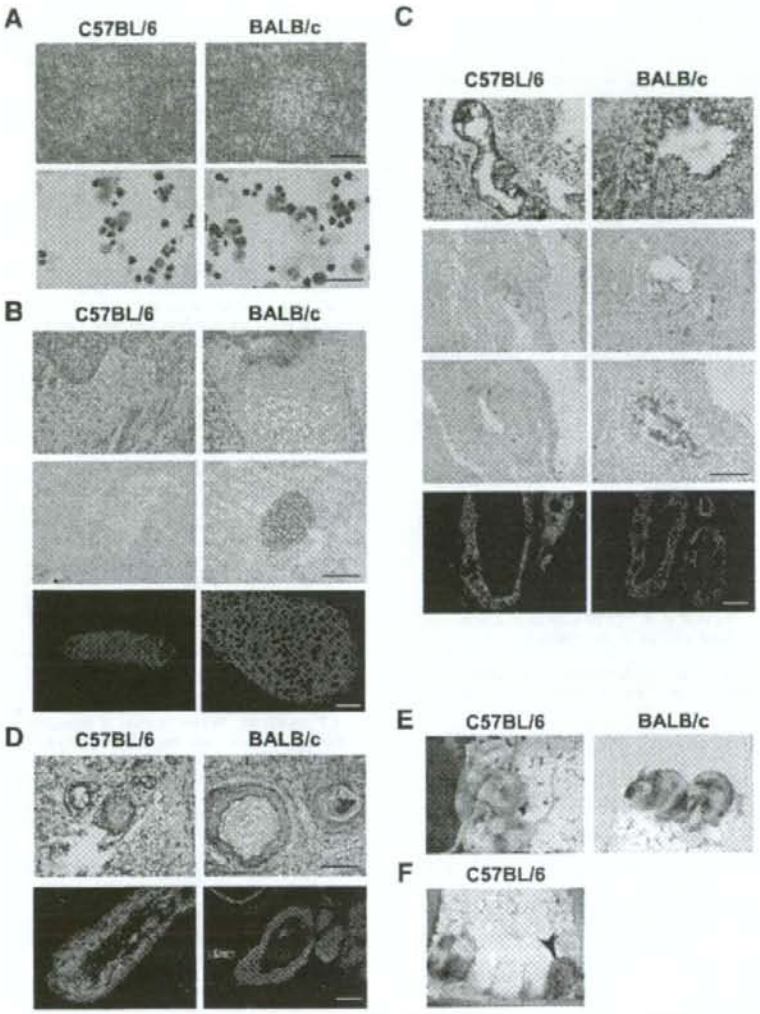

Figure 4. Multipotent differentiation capacity of embryonic stem (ES) cells established in the presence of 6-bromoindirubin-3'-oxime. **(A):** Hematopoietic differentiation capacities. The established ES cell lines were applied to an in vitro hematopoietic cell differentiation system using OP9 stromal cells. ES cells derived from both the C57BL/6 (left column) and BALB/c (right column) mice generated mesodermal colonies by day 5 (top) and differentiated to a variety of hematopoietic cells by day 12 (bottom) after differentiation induction. Scale bar = 40 μm. **(B–D):** Teratomas generated from the established ES cell lines. The ES cell lines from C57BL/6 (left column) and BALB/c (right column) mouse strains were injected under the skin of nude mice. After 3 weeks, the teratomas contained various tissues, including cartilage **(B)** (H&E, Alcian Blue, and anti-type II collagen staining), mucosal glands **(C)** (H&E, periodic acid-Schiff, Alcian Blue, and anti-cytokeratin staining), and squamous epithelium **(D)** (H&E and anti-cytokeratin staining). Scale bars = 100 μm. **(E):** Production of chimeric mice using the established ES cells. ES cells derived from C57BL/6 mice (black coat) were injected into blastocysts of BALB/c mice (white coat; left) or ES cells derived from BALB/c mice were injected into blastocysts of C57BL/6 mice (right). **(F):** Germline transmission of a C57BL/6 ES cell line. Chimeras obtained after injection of the C57BL/6 ES cells into BALB/c blastocysts were crossed to ICR mice. Germline transmission of the C57BL/6 cells was demonstrated by the birth of offspring with agouti coat color (arrowhead; details are given in Materials and Methods).

blastocysts that had been treated with BIO from the two-cell stage (data not shown). In contrast, Akt activation did not inhibit the outgrowth of endodermal cells in isolated ICM culture (supplemental online Fig. 1). Thus, in addition to its supporting effect on epiblasts, inhibition of GSK-3 with BIO treatment may improve ES cell derivation via inhibition of endodermal proliferation.

In this study, we revealed that ES cells can be established efficiently not only from permissive but also from refractory mouse strains using BIO treatment. Availability of ES cells derived from various mouse strains with genetic disorders and alterations will help us understand the complex genetic networks underlying human diseases and developmental processes. Self-renewal of ES cells is supported by BIO treatment in both mice and humans [11], indicating that GSK-3 plays an evolutionarily conserved role in the regulation of ES cell pluripotency. Hence, this strategy is potentially applica-

Downloaded from www.StemCells.com at Keio University Shinanomachi Media Center on March 6, 2008

ble to ES cell derivation in various mammalian species, including humans.

Acknowledgments

We thank Dr. E. Morii for advices on histological analysis and A. Kawai and Y. Koreeda for production of chimeric mice. This work was supported in part by grants from the Ministry of Education, Science, Sports and Culture; Astellas Foundation for Research on Metabolic Disorders; and the 21st Century Center of Excellence, Center for Integrated Cell and Tissue Regulation.

Disclosure of Potential Conflicts of Interest

The authors indicate no potential conflicts of interest.

References

1 Prelle K, Zink N, Wolf E. Pluripotent stem cells—Model of embryonic development, tool for gene targeting, and basis of cell therapy. Anat Histol Embryol 2002;31:169–186.
2 Wobus AM, Boheler KR. Embryonic stem cells: Prospects for developmental biology and cell therapy. Physiol Rev 2005;85:635–678.
3 Hoffman LM, Carpenter MK. Characterization and culture of human embryonic stem cells. Nat Biotechnol 2005;23:699–708.
4 Kawase E, Suemori H, Takahashi N et al. Strain difference in establishment of mouse embryonic stem (ES) cell lines. Int J Dev Biol 1994;38:385–390.
5 Schoonjans L, Kreemers V, Danloy S et al. Improved generation of germline-competent embryonic stem cell lines from inbred mouse strains. STEM CELLS 2003;21:90–97.
6 Boeuf H, Hauss C, Graeve FD et al. Leukemia inhibitory factor-dependent transcriptional activation in embryonic stem cells. J Cell Biol 1997;138:1207–1217.
7 Matsuda T, Nakamura T, Nakao K et al. STAT3 activation is sufficient to maintain an undifferentiated state of mouse embryonic stem cells. EMBO J 1999;18:4261–4269.
8 Niwa H, Burdon T, Chambers I et al. Self-renewal of pluripotent embryonic stem cells is mediated via activation of STAT3. Genes Dev 1998;12:2048–2060.
9 Humphrey RK, Beattie GM, Lopez AD et al. Maintenance of pluripotency in human embryonic stem cells is STAT3 independent. STEM CELLS 2004;22:522–530.
10 Sumi T, Fujimoto Y, Nakatsuji N et al. STAT3 is dispensable for maintenance of self-renewal in nonhuman primate embryonic stem cells. STEM CELLS 2004;22:861–872.
11 Sato N, Meijer L, Skaltsounis L et al. Maintenance of pluripotency in human and mouse embryonic stem cells through activation of Wnt signaling by a pharmacological GSK-3-specific inhibitor. Nat Med 2004;10:55–63.
12 Dravid G, Ye Z, Hammond H et al. Defining the role of Wnt/beta-catenin signaling in the survival, proliferation, and self-renewal of human embryonic stem cells. STEM CELLS 2005;23:1489–1501.
13 Ogawa K, Nishinakamura R, Iwamatsu Y et al. Synergistic action of Wnt and LIF in maintaining pluripotency of mouse ES cells. Biochem Biophys Res Commun 2006;343:159–166.
14 Paling NR, Wheadon H, Bone HK et al. Regulation of embryonic stem cell self-renewal by phosphoinositide 3-kinase-dependent signaling. J Biol Chem 2004;279:48063–48070.
15 Watanabe S, Umehara H, Murayama K et al. Activation of Akt signaling is sufficient to maintain pluripotency in mouse and primate embryonic stem cells. Oncogene 2006;25:2697–2707.
16 Boiani M, Scholer HR. Regulatory networks in embryo-derived pluripotent stem cells. Nat Rev Mol Cell Biol 2005;6:872–884.
17 Niwa H. How is pluripotency determined and maintained? Development 2007;134:635–646.
18 Murayama K, Kimura T, Tarutani M et al. Akt activation induces epidermal hyperplasia and proliferation of epidermal progenitors. Oncogene 2007;26:4882–4888.
19 Solter D, Knowles BB. Immunosurgery of mouse blastocyst. Proc Natl Acad Sci U S A 1975;72:5099–5102.
20 Nakano T, Kodama H, Honjo T. In vitro development of primitive and definitive erythrocytes from different precursors. Science 1996;272:722–724.
21 Kimura T, Ito C, Watanabe S et al. Mouse Germ cell-less as an essential component for nuclear integrity. Mol Cell Biol 2003;23:1304–1315.
22 Meijer L, Skaltsounis AL, Magiatis P et al. GSK-3-selective inhibitors derived from Tyrian purple indirubins. Chem Biol 2003;10:1255–1266.
23 Noben-Trauth N, Kohler G, Burki K et al. Efficient targeting of the IL-4 gene in a BALB/c embryonic stem cell line. Transgenic Res 1996;5:487–491.
24 Doble BW, Woodgett JR. GSK-3: Tricks of the trade for a multi-tasking kinase. J Cell Sci 2003;116:1175–1186.
25 Jope RS, Johnson GV. The glamour and gloom of glycogen synthase kinase-3. Trends Biochem Sci 2004;29:95–102.
26 Ahn S, Joyner AL. In vivo analysis of quiescent adult neural stem cells responding to Sonic hedgehog. Nature 2005;437:894–897.
27 Androutsellis-Theotokis A, Leker RR, Soldner F et al. Notch signalling regulates stem cell numbers in vitro and in vivo. Nature 2006;442:823–826.
28 Clement V, Sanchez P, de Tribolet N et al. HEDGEHOG-GLI1 signaling regulates human glioma growth, cancer stem cell self-renewal, and tumorigenicity. Curr Biol 2007;17:165–172.
29 Karhadkar SS, Bova GS, Abdallah N et al. Hedgehog signalling in prostate regeneration, neoplasia and metastasis. Nature 2004;431:707–712.
30 Varnum-Finney B, Xu L, Brashem-Stein C et al. Pluripotent, cytokine-dependent, hematopoietic stem cells are immortalized by constitutive Notch1 signaling. Nat Med 2000;6:1278–1281.
31 Cartwright P, McLean C, Sheppard A et al. LIF/STAT3 controls ES cell self-renewal and pluripotency by a Myc-dependent mechanism. Development 2005;132:885–896.
32 Takahashi K, Yamanaka S. Induction of pluripotent stem cells from mouse embryonic and adult fibroblast cultures by defined factors. Cell 2006;126:663–676.

See www.StemCells.com for supplemental material available online.

Downloaded from www.StemCells.com at Keio University Shinanomachi Media Center on March 6, 2008

Cell. Mol. Life Sci. 64 (2007) 1945 – 1958
1420-682X/07/151945-14
DOI 10.1007/s00018-007-7037-7
© Birkhäuser Verlag, Basel, 2007

Cellular and Molecular Life Sciences

Review

Mechanisms of sperm-egg interactions emerging from gene-manipulated animals

M. Okabe[a, *] and J. M. Cummins[b]

[a] Genome Information Research Center, Research Institute for Microbial Diseases, Osaka University, Yamadaoka 3-1, Suita, Osaka, 565-0871 (Japan), Fax: +81 6 6879 8376, e-mail: okabe@gen-info.osaka-u.ac.jp
[b] Anatomy, School of Health Sciences VB 1:10, Murdoch University, Murdoch (Australia)

Received 26 January 2007; received after revision 7 March 2007; accepted 17 April 2007
Online First 11 June 2007

Abstract. Untangling the molecular nature of sperm-egg interactions is fundamental if we are to understand fertilization. These phenomena have been studied for many years using biochemical approaches such as antibodies and ligands that interact with sperm or with eggs and their vestments. However, when homologous genetic recombination techniques were applied, most of the phenotypic factors of the gene-manipulated animals believed "essential" for fertilization were found to be dispensable. Of course, all biological systems contain redundancies and compensatory mechanisms, but as a whole the old model of fertilization clearly requires significant modification. In this review, we use the results of gene manipulation experiments in animals to propose the basis for a new vision.

Keywords. Fertilization, sperm-egg interaction, gene manipulation, zona pellucida.

Introduction

Living creatures developed the basic structures for ears before they had any way to sense sound and have crafted eyes as sensors for light at least 40 times using a common genetic toolkit [1]. They even invented lenses without any knowledge of physics and succeeded in projecting images of the environment on retinas. They developed means of sensing chemicals in the environment that we recognize today as the ability to smell and taste. About a billion years ago, the ancestors of today's eukaryotic organisms also devised sex [2]: a genetic shuffling and exchange mechanism that functions still as one of evolution's major Generators of Diversity. Originally, there was little disparity in size between the different gamete types, and some organisms such as fungi and protists had – and still have – multiple genders, so the terms "male" and "female" are meaningless for them. One problem the gametes had to overcome was that of finding each other. Not surprisingly, they used chemical sensing, and we now realize that gamete detection mechanisms are still closely related to those used in smell and taste. With the evolution of multicellularity, a division of labor arose. Chordates developed an alternating haploid/diploid life cycle, with the diploid somatic phase dominant and the haploid phase limited to the much smaller gametes. The gametes themselves diverged in form and function, with the male sperm becoming a tiny motile genetic dispersal machine and the female egg remaining as a largely passive recipient carrying the resources needed to fuel early embryonic development [3]. In fact, the terms "male" and "female" are defined by the type of gamete an individual soma produces rather than the specific

* Corresponding author.